Structural Engineering and Mechanics, *Vol. 75, No. 2 (2020) 247-269*
DOI: https://doi.org/10.12989/sem.2020.75.2.247

Analysis of laminated composite plates based on different shear deformation plate theories

Hojat Tanzadeh and Hossein Amoushahi*

Department of Civil and Transportation Engineering, University of Isfahan, Isfahan 81746-73441, Iran

(Received January 21, 2019, Revised April 15, 2019, Accepted February 21, 2020)

Abstract. A finite strip formulation was developed for buckling and free vibration analysis of laminated composite plates based on different shear deformation plate theories. The different shear deformation theories such as Zigzag higher order, Refined Plate Theory (RPT) and other higher order plate theories by variation of transverse shear strains through plate thickness in the parabolic form, sine and exponential were adopted here. The two loaded opposite edges of the plate were assumed to be simply supported and remaining edges were assumed to have arbitrary boundary conditions. The polynomial shape functions are applied to assess the in-plane and out-of-plane deflection and rotation of the normal cross-section of plates in the transverse direction. The finite strip procedure based on the virtual work principle was applied to derive the stiffness, geometric and mass matrices. Numerical results were obtained based on various shear deformation plate theories to verify the proposed formulation. The effects of length to thickness ratios, modulus ratios, boundary conditions, the number of layers and fiber orientation of cross-ply and angle-ply laminates were determined. The additional results on the same effects in the interaction of biaxial in-plane loadings on the critical buckling load were determined as well.

Keywords: buckling; free vibration; laminated plates; zigzag; refined plate theory

1. Introduction

The plates made of composite materials require accurate structural analysis to predict the correct behavior. Laminated composite plates have been and are being extensively applied as structural members. To take advantage of all potential of laminated composite members, developing the reliable and practical models to accurately predict the buckling and free vibration behaviors of these structures that are being applied in the modern aircraft and aerospace industry, marine vessels, pipes, and pressure vessels are necessary. Laminated composite plates due to their high strength-to-weight ratio, the high specific strengths, high durability subjected to fatigue loading, specific stiffnesses, etc., are of major interest. Running efficient analyses for composite structures is a major focus among many researchers.

Many equivalent single layer (ESL) plate theories with appropriate assumptions were proposed to transform the 3D problem into a 2D one. Among the ESL plate theories, the classical laminated plate theory (CLPT) and first-order shear deformation theory (FSDT) were developed for the analysis of thin and moderately thick plates. The FSDT requires a shear correction coefficient to meet free boundary conditions on the lower and upper surface of the plates. Therefore, higher order shear deformation theories were proposed by the researchers, to avoid shear correction coefficient application.

One of the most common HSDT theories was third-order shear deformation theory (TSDT) presented by Reddy (2004) where a parabolic variation of the transverse shear strains through the plate thickness, accounted zero transverse shear stresses on the top and bottom surfaces of the plates. Afterward, Touratier (1991) proposedtrigonometric shear deformation theory, and Karama *et al.* (2003) introduced an exponential shear deformation theory, for in-plane displacement in the thickness. A refined plate theory was proposed by Shimpi *et al.* (2002) where the displacement field involved fewer unknowns in the equations in comparison with the higher order deformation theories. This theory became similar to the CLPT theory when the shear component was eliminated.

To predict the behavior of laminated plate in an accurate sense, there exist many laminated plate theories. As to for the shear stress continuity across each layer interface, these theories were not formulated, therefore the accuracy analyses must be run. Cho and Parmerter (1993) developed a higher-order zigzag laminate theory, where parabolic variation was considered through the thickness of the plate for transverse shear strains, and for shear stress continuity across each layer interface the zigzag theory was considered for the strain discontinuities required for stress continuity. Thus, the number of involved unknowns remained the same, but a continuous distribution of shear stresses was achieved, in a sense that the accuracy of analyses was significantly improved with only limited additional calculations. Sreehari *et al.* (2016) developed a finite element formulation based on Inverse Hyperbolic Shear Deformation Theory (IHSDT) for bending and buckling analyses of smart composite plates. By considering a smart structure with piezoelectric material perfectly bonded to the

*Corresponding author, Ph.D.
E-mail: h.amoushahi@eng.ui.ac.ir

http://www.techno-press.com/journals/sem&subpage=7 ISSN: 1225-4568 (Print), 1598-6217 (Online)

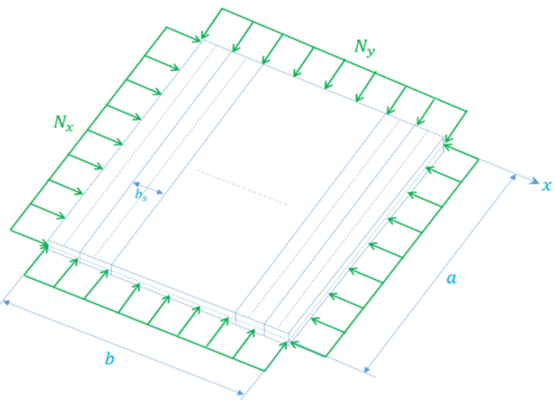

(a) External in-plane loads in a rectangular plate

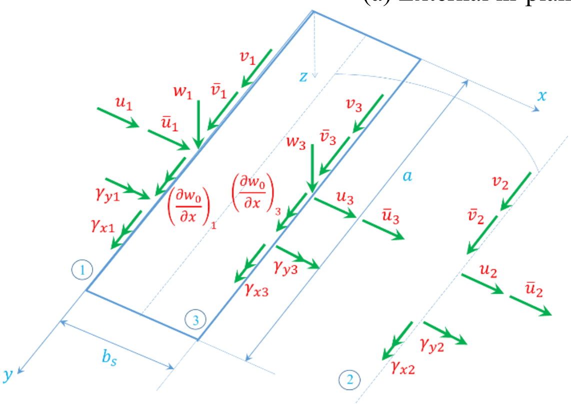

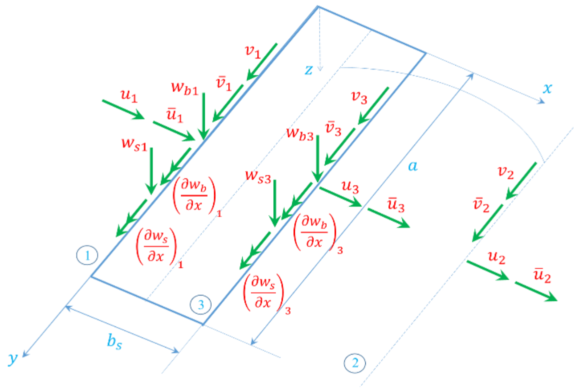

(b) Higher-order shear deformation theories (c) Refined plate theory

Fig. 1 The DOFs of a finite strip element based on HSDT and RPT

top and the bottom surface of a laminated composite plate, they yield the governing equation of a piezolaminated composite plate through Hamilton's variational principle. Sayyad *et al.* (2016) applied a simple trigonometric shear deformation theory with four unknown variables to assess the bending, buckling and free vibration of cross-ply laminated composite plates. To consider the shear deformation effect, they applied sinusoidal function in terms of thickness coordinate that transverse displacement consisted of bending and shear components. Singh and Singh (2017) developed two new shear deformation theories named Trigonometric Deformation Theory (TDT) and Trigonometric Hyperbolic Deformation Theory (THDT) for the analysis of laminated and three-dimensional braided composite plates.

By applying a refined simple n$^{\text{th}}$-higher–order shear deformation theory, the vibration behavior of simply supported composite rectangular plates were assessed by Bouazza *et al.* (2017). Governing equations were devised through Hamilton's principle based on closed-form solution by applying the Navier's technique. Aydogdu and Aksencer (2018) formulated the buckling of composite plates based on first-order and third-order shear deformation plate theories with linearly varying in-plane loads through the Ritz method with simple polynomials in the displacement field. Loaded edges were assumed as being simply supported and the remaining ones were arbitrary. They modified displacement field components meet the continuity of transverse stresses among the layers of cross-ply symmetric lay-up composite plates. By applying the Reddy's TSDT and Eringen's nonlocality, the nonlocal nonlinear finite element analysis of laminated composite plates was presented by Raghu *et al.* (2018). They applied four–noded rectangular conforming element with eight degrees of freedom per node. By applying the Eringen's stress gradient constitutive model, the governing equations of the third-order shear deformation theory with the von Karman strains were derived. Fallah and Delzendeh (2018) proposed a new meshless finite volume (MFV) method and applied the first-order shear deformation theory (FSDT) in the formulation for free vibration analysis of laminated composite plates. To approximate the field variables in their study, moving least square approximation (MLS) technique was applied.

The ordinary finite strip method (FSM) was applied in this article for buckling and free vibration analysis of composite laminated plates based on different shear deformation plate theories. The finite strip method, first introduced by Cheung (1968), to study the behavior of the structural element subjected to different loads and boundary conditions. The FSM is of lower degrees of freedom in comparison with other methods like finite element, finite layer, and spline finite strip method applied by researchers in their assessments.

The finite strip method is applied for stability, static and free vibration analysis of rectangular composite plates by authors (Amoushahi 2018, Amoushahi and Lajevardi 2018, Amoushahi and Goodarzian 2018, Tanzadeh and Amoushahi 2018) and (Akhras and Li 2007). The results indicate that, although the FEM is a powerful tool plate problems analysis, it is not economically feasible with rectangular plates. Akhras and Li (2007) developed stability, static and vibration analysis of laminated composite plates by spline finite strip method based on TSDT and zigzag plate theory for the elastic analysis of laminated composite plates. They assessed the static, free vibration and buckling analyses of laminated composite plates, while they did not assess the same based on zigzag theory and higher order theories with different variation in thickness of the plate. Also, in this study, the FSM formulation is written for analysis of cross-ply and angle-ply laminated plates based on refined plate theory (RPT) for the different variation of the transverse shear strains through the plate thickness. So, the finite strip method is applied to study buckling and free vibration analysis of laminated composite plates based on different plate deformation theories. Therefore, the finite strip formulation would be derived for the laminated plate in Section 2. So, by verifying the accuracy of results, the numerical results would be presented in Section 3. Finally, some concluding remarks are presented in Section 4.

2. Finite strip formulation of laminated plates

2.1 Kinematics of deformation

The ordinary finite strip method is considered for the analysis of rectangular laminated composite plates where two opposite edges in the longitudinal directions are assumed to be simply supported. The other two edges in the transverse direction can have arbitrary boundary conditions. The displacement functions are assumed to be polynomials in the transverse direction while in the longitudinal direction the trigonometric basic functions are considered. This approach allows the discretization of the rectangular plate in finite longitudinal strips based on different shear deformation theories, as shown in Fig. 1.

As observed in Fig. 1, the in-plane displacements u and v, lateral displacement w, the rotations of the normals to the midplane about the y and x axes, γ_x and γ_y respectively, are at each nodal line. The lateral displacement w based on refined plate theory has both the bending component w_b and the shear component w_s, where both are the functions of x and y coordinates. These parameters can be expressed in terms of the generalized displacement parameters as:

$$u_0 = \sum_{m=1}^{r}\sum_{i=1}^{3}\left[N_i(x)Y_{1m}(y)u_{im} + N_i(x)Y_{2m}(y)\bar{u}_{im}\right] \quad (1)$$

$$v_0 = \sum_{m=1}^{r}\sum_{i=1}^{3}\left[N_i(x)Y_{2m}(y)v_{im} + N_i(x)Y_{1m}(y)\bar{v}_{im}\right] \quad (2)$$

$$w_0 = \sum_{m=1}^{r}\sum_{i=1,3}\left[W_i(x)Y_{1m}(y)w_{im} + R_i(x)Y_{1m}(y)\left(\frac{\partial w}{\partial x}\right)_{im}\right] \quad (3)$$

$$w_b = \sum_{m=1}^{r}\sum_{i=1,3}\left[W_i(x)Y_{1m}(y)(w_b)_{im} + R_i(x)Y_{1m}(y)\left(\frac{\partial w_b}{\partial x}\right)_{im}\right] \quad (4)$$

$$w_s = \sum_{m=1}^{r}\sum_{i=1,3}\left[W_i(x)Y_{1m}(y)(w_s)_{im} + R_i(x)Y_{1m}(y)\left(\frac{\partial w_s}{\partial x}\right)_{im}\right] \quad (5)$$

$$\gamma_x = \sum_{m=1}^{r}\sum_{i=1}^{3} N_i(x)Y_{1m}(y)(\gamma_x)_{im} \quad (6)$$

$$\gamma_y = \sum_{m=1}^{r}\sum_{i=1}^{3} N_i(x)Y_{2m}(y)(\gamma_y)_{im} \quad (7)$$

where r is the number of longitudinal half-wavelengths. The specific forms of Y_{1m} and Y_{2m} for simply supported boundary conditions are considered to be $\sin(m\pi y/a)$ and$\cos(m\pi y/a)$, respectively. The displacement functions are assumed to be polynomials in the transverse direction, while, in the longitudinal direction, the trigonometric basic functions are applied. The $N_i(x)$ for $i = 1,2,3$ are the quadratic interpolation functions expressed as:

$$N_1(x) = 1 - 3\frac{x}{b_s} + 2\frac{x^2}{b_s^2} \quad N_2(x) = 4\frac{x}{b_s} - 4\frac{x^2}{b_s^2} \quad N_3(x) = 2\frac{x^2}{b_s^2} - \frac{x}{b_s} \quad (8)$$

Parameter b_s is the strip width and $W_i(x)$ and $R_i(x)$ for $i = 1,3$ are the following Hermitian cubic polynomials:

$$W_1(x) = 1 - 3\frac{x^2}{b_s^2} + 2\frac{x^3}{b_s^3} \quad W_3(x) = 3\frac{x^2}{b_s^2} - 2\frac{x^3}{b_s^3} \quad R_1(x) = -x + 2\frac{x^2}{b_s} - \frac{x^3}{b_s^2} \quad R_3(x) = \frac{x^2}{b_s} - \frac{x^3}{b_s^2} \quad (9)$$

The DOF vector for each finite strip could be expressed as:

$$\boldsymbol{\Delta} = [\boldsymbol{\Delta}_{m=1} \quad \boldsymbol{\Delta}_{m=2} \quad \cdots \quad \boldsymbol{\Delta}_{m=r}]^T; \quad \boldsymbol{\Delta}_m = [\boldsymbol{\Delta}_{1m} \quad \boldsymbol{\Delta}_{2m} \quad \boldsymbol{\Delta}_{3m}]^T \quad (10)$$

where $\boldsymbol{\Delta}_m$ is the DOF vector of one strip of three lines with an equal spaced nodal line in m^{th} mode. In Eq. (10), $\boldsymbol{\Delta}_{im}$ for $i = 1,2,3$ (i is the nodal line number) is written as Eq. (11) for HSDT and Eq. (12) for RPT.

$$\begin{aligned}\boldsymbol{\Delta}_{1m} &= \left[u_1 \quad \bar{u}_1 \quad v_1 \quad \bar{v}_1 \quad w_1 \quad \left(\frac{\partial w}{\partial x}\right)_1 \quad \gamma_{x1} \quad \gamma_{y1}\right]_m^T \\ \boldsymbol{\Delta}_{2m} &= [u_2 \quad \bar{u}_2 \quad v_2 \quad \bar{v}_2 \quad \gamma_{x2} \quad \gamma_{y2}]_m^T \\ \boldsymbol{\Delta}_{3m} &= \left[u_3 \quad \bar{u}_3 \quad v_3 \quad \bar{v}_3 \quad w_3 \quad \left(\frac{\partial w}{\partial x}\right)_3 \quad \gamma_{x3} \quad \gamma_{y3}\right]_m^T\end{aligned} \quad (11)$$

$$\begin{aligned}\boldsymbol{\Delta}_{1m} &= \left[u_1 \quad \bar{u}_1 \quad v_1 \quad \bar{v}_1 \quad (w_b)_1 \quad \left(\frac{\partial w_b}{\partial x}\right)_1 \quad (w_s)_1 \quad \left(\frac{\partial w_s}{\partial x}\right)_1\right]_m^T \\ \boldsymbol{\Delta}_{2m} &= [u_2 \quad \bar{u}_2 \quad v_2 \quad \bar{v}_2]_m^T \\ \boldsymbol{\Delta}_{3m} &= \left[u_3 \quad \bar{u}_3 \quad v_3 \quad \bar{v}_3 \quad (w_b)_3 \quad \left(\frac{\partial w_b}{\partial x}\right)_3 \quad (w_s)_3 \quad \left(\frac{\partial w_s}{\partial x}\right)_3\right]_m^T\end{aligned} \quad (12)$$

where u_i, $\bar{u}_i$, v_i, $\bar{v}_i$, and w_i are the displacement components, Fig. 1, γ_{xi} and γ_{yi} are the transverse shear deformation measured at the midplane. The $(w_b)_i$ and $(w_s)_i$ are the bending and shear components based on RPT.

The analysis here is run based on Reddy's third-order shear deformation (Reddy 2004), Touratier's Sine (Touratier 1991), Afaq's exponential (Karama *et al.* 2003), zigzag laminate (Cho and Parmerter 1993) and refined plate theory (RPT), (Shimpi 2002) theories for different variations of shear in thickness. Based on these theories, displacement functions u, v and w at any x, y, z point of the laminate have the following relations with the mid-plane displacements:

$$\begin{cases} \text{for all theories:} \\ \mathbf{u}(x,y,z) = \mathbf{u}_0(x,y) + z\overline{\mathbf{w}}(x,y) + \mathbf{F}(z)\overline{\gamma}(x,y) \\ \text{for RPT: } w(x,y,z) = w_b(x,y) + w_s(x,y) \\ \text{for other theories: } w(x,y,z) = w_0(x,y) \end{cases} \tag{13}$$

where

$$\mathbf{u} = \begin{Bmatrix} u \\ v \end{Bmatrix}; \mathbf{u}_0 = \begin{Bmatrix} u_0 \\ v_0 \end{Bmatrix}; \overline{\mathbf{w}} = \begin{Bmatrix} -\overline{w}_1 \\ -\overline{w}_2 \end{Bmatrix}; \overline{\gamma} = \begin{Bmatrix} \overline{\gamma}_1 \\ \overline{\gamma}_2 \end{Bmatrix};$$
$$\mathbf{F}(z) = \begin{bmatrix} F(z)_{11} & F(z)_{12} \\ F(z)_{21} & F(z)_{22} \end{bmatrix} \tag{14}$$

And the other components such as $\overline{\mathbf{w}}$, $\overline{\gamma}$, and $\mathbf{F}(z)$ are tabulated in Table 1.

The generalized displacements have the following linear relations with the generalized strains:

$$\varepsilon = \langle \varepsilon_x \quad \varepsilon_y \quad \gamma_{xy} \rangle^{\mathrm{T}} = \left\langle \frac{\partial u}{\partial x} \quad \frac{\partial v}{\partial y} \quad \frac{\partial u}{\partial y} + \frac{\partial v}{\partial x} \right\rangle^{\mathrm{T}};$$
$$\gamma = \langle \gamma_{yz} \quad \gamma_{xz} \rangle^{\mathrm{T}} = \left\langle \frac{\partial v}{\partial z} + \frac{\partial w}{\partial y} \quad \frac{\partial u}{\partial z} + \frac{\partial w}{\partial x} \right\rangle^{\mathrm{T}} \tag{15}$$

Bending and shear strains in Eq. (15) based on components of Table 1 are written as:

$$\begin{aligned} \varepsilon &= \varepsilon_0 + z\kappa \\ &+ F(z)_{11}\chi_{\mathbf{a}} + F(z)_{22}\chi_{\mathbf{b}} + F(z)_{12}\chi_{\mathbf{c}} + F(z)_{21}\chi_{\mathbf{d}} \\ &= \left\langle \frac{\partial u_0}{\partial x} \quad \frac{\partial v_0}{\partial y} \quad \frac{\partial u_0}{\partial y} + \frac{\partial v_0}{\partial x} \right\rangle^{\mathrm{T}} \\ &+ z\left\langle -\frac{\partial \overline{w}_1}{\partial x} \quad -\frac{\partial \overline{w}_2}{\partial y} \quad -2\frac{\partial \overline{w}_1}{\partial y} \text{ or } -2\frac{\partial \overline{w}_2}{\partial x} \right\rangle^{\mathrm{T}} \\ &+ F(z)_{11}\left\langle \frac{\partial \overline{\gamma}_1}{\partial x} \quad 0 \quad \frac{\partial \overline{\gamma}_1}{\partial y} \right\rangle^{\mathrm{T}} + F(z)_{22}\left\langle 0 \quad \frac{\partial \overline{\gamma}_2}{\partial y} \quad \frac{\partial \overline{\gamma}_2}{\partial x} \right\rangle^{\mathrm{T}} \\ &+ F(z)_{12}\left\langle \frac{\partial \overline{\gamma}_2}{\partial x} \quad 0 \quad \frac{\partial \overline{\gamma}_2}{\partial y} \right\rangle^{\mathrm{T}} + F(z)_{21}\left\langle 0 \quad \frac{\partial \overline{\gamma}_1}{\partial y} \quad \frac{\partial \overline{\gamma}_1}{\partial x} \right\rangle^{\mathrm{T}} \end{aligned} \tag{16}$$

$$\begin{aligned} \gamma &= \frac{\partial F(z)_{11}}{\partial z}\gamma_{\mathbf{a}} + \frac{\partial F(z)_{22}}{\partial z}\gamma_{\mathbf{b}} \\ &+ \frac{\partial F(z)_{12}}{\partial z}\gamma_{\mathbf{c}} + \frac{\partial F(z)_{21}}{\partial z}\gamma_{\mathbf{d}} \\ &= \frac{\partial F(z)_{11}}{\partial z}\langle 0 \quad \overline{\gamma}_1 \rangle^{\mathrm{T}} + \frac{\partial F(z)_{22}}{\partial z}\langle \overline{\gamma}_2 \quad 0 \rangle^{\mathrm{T}} \\ &+ \frac{\partial F(z)_{12}}{\partial z}\langle 0 \quad \overline{\gamma}_2 \rangle^{\mathrm{T}} + \frac{\partial F(z)_{21}}{\partial z}\langle \overline{\gamma}_1 \quad 0 \rangle^{\mathrm{T}} \end{aligned} \tag{17}$$

Parameter ε_0 is the in-plane strain vector, κ is the curvature vector, $\chi_{\mathbf{a}}$ and alike, constitute the different portions of the bending strain vector and $\gamma_{\mathbf{a}}$ and alike constitute the different portions of the shear strain vector. By inserting different components of Table 1 in Eq. (16) and Eq. (17), the bending and the strain vectors for different plate theories are yield. By applying Eqs. (1)-(7), (16) and (17), the components of bending and shear strain vectors are rewritten based on the finite strip method expressed as:

$$\begin{Bmatrix} \varepsilon_0 \\ \kappa \\ \chi_{\mathbf{a}} \\ \chi_{\mathbf{b}} \\ \chi_{\mathbf{c}} \\ \chi_{\mathbf{d}} \end{Bmatrix} = \sum_{m=1}^{r} \begin{Bmatrix} \mathbf{B}_m^{\mathbf{b}\varepsilon_0} \\ \mathbf{B}_m^{\mathbf{b}\kappa} \\ \mathbf{B}_m^{\mathbf{b}\chi_{\mathbf{a}}} \\ \mathbf{B}_m^{\mathbf{b}\chi_{\mathbf{b}}} \\ \mathbf{B}_m^{\mathbf{b}\chi_{\mathbf{c}}} \\ \mathbf{B}_m^{\mathbf{b}\chi_{\mathbf{d}}} \end{Bmatrix} \mathbf{\Delta}_m = \sum_{m=1}^{r} \mathbf{B}_m^{\mathbf{b}}\mathbf{\Delta}_m = \mathbf{B}^{\mathbf{b}}\mathbf{\Delta}; \tag{18}$$
$$\mathbf{B}^{\mathbf{b}} = [\mathbf{B}_1^{\mathbf{b}} \quad \mathbf{B}_2^{\mathbf{b}} \quad \dots \quad \mathbf{B}_r^{\mathbf{b}}]$$

$$\begin{Bmatrix} \gamma_{\mathbf{a}} \\ \gamma_{\mathbf{b}} \\ \gamma_{\mathbf{c}} \\ \gamma_{\mathbf{d}} \end{Bmatrix} = \sum_{m=1}^{r} \begin{Bmatrix} \mathbf{B}_m^{\mathbf{s}\gamma_{\mathbf{a}}} \\ \mathbf{B}_m^{\mathbf{s}\gamma_{\mathbf{b}}} \\ \mathbf{B}_m^{\mathbf{s}\gamma_{\mathbf{c}}} \\ \mathbf{B}_m^{\mathbf{s}\gamma_{\mathbf{d}}} \end{Bmatrix} \mathbf{\Delta}_m = \sum_{m=1}^{r} \mathbf{B}_m^{\mathbf{s}}\mathbf{\Delta}_m = \mathbf{B}^{\mathbf{s}}\mathbf{\Delta}; \tag{19}$$
$$\mathbf{B}^{\mathbf{s}} = [\mathbf{B}_1^{\mathbf{s}} \quad \mathbf{B}_2^{\mathbf{s}} \quad \dots \quad \mathbf{B}_r^{\mathbf{s}}]$$

where the matrices $\mathbf{B}_m^{\mathbf{b}\alpha}$ for $\alpha = \varepsilon_0, \kappa, \chi_a, \chi_b, \chi_c, \chi_d$ and $\mathbf{B}_m^{\mathbf{s}\beta}$ for $\beta = \gamma_a, \gamma_b, \gamma_c, \gamma_d$ are formed by applying the three matrices of each line as:

$$\mathbf{B}_m^{\mathbf{b}\alpha} = [\mathbf{B}_{1m}^{\mathbf{b}\alpha} \quad \mathbf{B}_{2m}^{\mathbf{b}\alpha} \quad \mathbf{B}_{3m}^{\mathbf{b}\alpha}]; (\alpha = \varepsilon_0, \kappa, \chi_a, \chi_b, \chi_c, \chi_d) \tag{20}$$

$$\mathbf{B}_m^{\mathbf{s}\beta} = [\mathbf{B}_{1m}^{\mathbf{s}\beta} \quad \mathbf{B}_{2m}^{\mathbf{s}\beta} \quad \mathbf{B}_{3m}^{\mathbf{s}\beta}]; (\beta = \gamma_a, \gamma_b, \gamma_c, \gamma_d) \tag{21}$$

The matrices $\mathbf{B}_m^{\mathbf{b}\alpha}$ and $\mathbf{B}_m^{\mathbf{s}\beta}$ are expressed in Appendix A for different plate theories.

2.2 Stress and strain relationships

The stress-strain constitutive law for the material of each layer of laminate can be obtained in the following matrix:

$$\begin{Bmatrix} \sigma \\ \tau \end{Bmatrix}_{5\times1}^{(k)} = \begin{Bmatrix} \overline{\mathbf{Q}}_{\mathbf{b}} & \mathbf{0} \\ \mathbf{0} & \overline{\mathbf{Q}}_{\mathbf{s}} \end{Bmatrix}_{5\times5}^{(k)} \begin{Bmatrix} \varepsilon \\ \gamma \end{Bmatrix}_{5\times1}^{(k)} \tag{22}$$

where $\sigma^{(k)}$ and $\tau^{(k)}$ are the bending and shear stress, respectively, expressed as:

$$\sigma^{(k)} = \langle \sigma_x \quad \sigma_y \quad \sigma_{xy} \rangle^{\mathrm{T}}; \ \tau^{(k)} = \langle \tau_{yz} \quad \tau_{zx} \rangle^{\mathrm{T}} \tag{23}$$

Matrix $\overline{\mathbf{Q}}_{\mathbf{b}}^{(k)}$ is the reduced orthotropic elastic stiffness matrix and $\overline{\mathbf{Q}}_{\mathbf{s}}^{(k)}$ is the elastic coefficient of k^{th} layer for out-of-plane shear.

$$\overline{\mathbf{Q}}_{\mathbf{b}}^{(k)} = \begin{bmatrix} \overline{Q}_{11} & \overline{Q}_{12} & \overline{Q}_{16} \\ \overline{Q}_{12} & \overline{Q}_{22} & \overline{Q}_{16} \\ \overline{Q}_{16} & \overline{Q}_{26} & \overline{Q}_{66} \end{bmatrix}^{(k)}; \ \overline{\mathbf{Q}}_{\mathbf{s}}^{(k)} = \begin{bmatrix} \overline{Q}_{44} & \overline{Q}_{45} \\ \overline{Q}_{45} & \overline{Q}_{55} \end{bmatrix}^{(k)} \tag{24}$$

Table 1 Components of Eq. (14) based on different plate theories.

Theory	$\overline{w}_1$	$\overline{w}_2$	$\overline{\gamma}_1$	$\overline{\gamma}_2$	$F(z)_{11}$	$F(z)_{12}$	$F(z)_{21}$	$F(z)_{22}$
TSDT of Reddy (2004)	$\frac{\partial w_0}{\partial x}$	$\frac{\partial w_0}{\partial y}$	γ_x	γ_y	$z\left(1-\frac{4z^2}{3h^2}\right)$	0	0	$z\left(1-\frac{4z^2}{3h^2}\right)$
HSDT of Touratier (1991)	$\frac{\partial w_0}{\partial x}$	$\frac{\partial w_0}{\partial y}$	γ_x	γ_y	$\frac{h}{\pi}\sin\left(\frac{\pi z}{h}\right)$	0	0	$\frac{h}{\pi}\sin\left(\frac{\pi z}{h}\right)$
HSDT of Karama *et al.* (2003)	$\frac{\partial w_0}{\partial x}$	$\frac{\partial w_0}{\partial y}$	γ_x	γ_y	$z\exp(-2(z/h)^2)$	0	0	$z\exp(-2(z/h)^2)$
FSDT ($k_s=\frac{5}{6}$)	$\frac{\partial w_0}{\partial x}$	$\frac{\partial w_0}{\partial y}$	γ_x	γ_y	z	0	0	z
CLPT	$\frac{\partial w_0}{\partial x}$	$\frac{\partial w_0}{\partial y}$	—	—	0	0	0	0
RPT of Shimpi (2002)	$\frac{\partial w_b}{\partial x}$	$\frac{\partial w_b}{\partial y}$	$\frac{\partial w_s}{\partial x}$	$\frac{\partial w_s}{\partial y}$	$z\left[\frac{1}{4}-\frac{5}{3}(z/h)^2\right]$	0	0	$z\left[\frac{1}{4}-\frac{5}{3}(z/h)^2\right]$
RPT of Reddy (2004)	$\frac{\partial w_b}{\partial x}$	$\frac{\partial w_b}{\partial y}$	$\frac{\partial w_s}{\partial x}$	$\frac{\partial w_s}{\partial y}$	$\frac{-4z}{3}(z/h)^2$	0	0	$\frac{-4z}{3}(z/h)^2$
RPT of Touratier (1991)	$\frac{\partial w_b}{\partial x}$	$\frac{\partial w_b}{\partial y}$	$\frac{\partial w_s}{\partial x}$	$\frac{\partial w_s}{\partial y}$	$\frac{h}{\pi}\sin\left(\frac{\pi z}{h}\right)-z$	0	0	$\frac{h}{\pi}\sin\left(\frac{\pi z}{h}\right)-z$
RPT of Mechab (2002)	$\frac{\partial w_b}{\partial x}$	$\frac{\partial w_b}{\partial y}$	$\frac{\partial w_s}{\partial x}$	$\frac{\partial w_s}{\partial y}$	$-\frac{2z\sinh\left(\frac{z^2}{h^2}\right)}{2\sinh\left(\frac{1}{4}\right)+\cosh\left(\frac{1}{4}\right)}$	0	0	$-\frac{2z\sinh\left(\frac{z^2}{h^2}\right)}{2\sinh\left(\frac{1}{4}\right)+\cosh\left(\frac{1}{4}\right)}$
HSDT of Cho and Parmerter (1993)	$\frac{\partial w_0}{\partial x}$	$\frac{\partial w_0}{\partial y}$	γ_x	γ_y	$[\mathbf{F}(z)]_k=[\mathbf{F}_1]_k+z[\mathbf{F}_2]_k+z^2[\mathbf{F}_3]+z^3[\mathbf{F}_4]$ [a]			

[a] The matrices $[\mathbf{F}_i]_k$ are described in Akhras and Li (2007) for k^{th} layer.

where the components of $\overline{\mathbf{Q}}_{\mathbf{b}}$ and $\overline{\mathbf{Q}}_{\mathbf{s}}$ are defined in Akhras and Li (2007).

2.3 Virtual work equation

In the present study, the stiffness, geometric and mass matrices are yield based on virtual work equation ($\delta W_{int}^e = \delta W_{ext}^e$), where, δ is the variational operator, W_{int}^e is the internal work and W_{ext}^e is the external work for buckling and free vibration analysis expressed by:

$$\frac{1}{2}\int(\varepsilon^{\mathrm{T}}\sigma+\gamma^{\mathrm{T}}\tau)dV=\frac{1}{2}\int\mathbf{G_u}^{\mathrm{T}}\sigma_{\mathbf{0}}\mathbf{G_u}dV+\frac{1}{2}\int\mathbf{G_v}^{\mathrm{T}}\sigma_{\mathbf{0}}\mathbf{G_v}dV++\frac{1}{2}\int\mathbf{G_w}^{\mathrm{T}}\sigma_{\mathbf{0}}\mathbf{G_w}dV++\frac{1}{2}\int\mathbf{u}^{\mathrm{T}}\overline{\rho}\mathbf{u}dV+\frac{1}{2}\int w^{\mathrm{T}}\rho_0 w dV \tag{25}$$

where $\sigma_{\mathbf{0}}$ is the initial in–plane stress matrix expressed as:

$$\sigma_{\mathbf{0}}=\frac{1}{h}\begin{bmatrix}n_x & n_{xy}\\ n_{xy} & n_y\end{bmatrix} \tag{26}$$

where h is the total plate thickness. In Eq. (25), the vectors $\mathbf{G_u}$, $\mathbf{G_v}$ and $\mathbf{G_w}$ are described as:

$$\mathbf{G_u}=\varepsilon_1+z\kappa_1+F(z)_{11}\chi_1+F(z)_{12}\chi_2\Rightarrow$$

$$\begin{Bmatrix}\frac{\partial u}{\partial x}\\ \frac{\partial u}{\partial y}\end{Bmatrix}=\begin{Bmatrix}\frac{\partial u_0}{\partial x}\\ \frac{\partial u_0}{\partial y}\end{Bmatrix}+z\begin{Bmatrix}-\frac{\partial\overline{w}_1}{\partial x}\\ -\frac{\partial\overline{w}_1}{\partial y}\end{Bmatrix}+F(z)_{11}\begin{Bmatrix}\frac{\partial\overline{\gamma}_1}{\partial x}\\ \frac{\partial\overline{\gamma}_1}{\partial y}\end{Bmatrix}+F(z)_{12}\begin{Bmatrix}\frac{\partial\overline{\gamma}_2}{\partial x} & \frac{\partial\overline{\gamma}_2}{\partial y}\end{Bmatrix}^T \tag{27}$$

$$\mathbf{G_v}=\varepsilon_2+z\kappa_2+F(z)_{22}\chi_2+F(z)_{21}\chi_1\Rightarrow$$

$$\begin{Bmatrix}\frac{\partial v}{\partial x}\\ \frac{\partial v}{\partial y}\end{Bmatrix}=\begin{Bmatrix}\frac{\partial v_0}{\partial x}\\ \frac{\partial v_0}{\partial y}\end{Bmatrix}+z\begin{Bmatrix}-\frac{\partial\overline{w}_2}{\partial x}\\ -\frac{\partial\overline{w}_2}{\partial y}\end{Bmatrix}+F(z)_{22}\begin{Bmatrix}\frac{\partial\overline{\gamma}_2}{\partial x}\\ \frac{\partial\overline{\gamma}_2}{\partial y}\end{Bmatrix}+F(z)_{21}\begin{Bmatrix}\frac{\partial\overline{\gamma}_1}{\partial x} & \frac{\partial\overline{\gamma}_1}{\partial y}\end{Bmatrix}^T \tag{28}$$

$$\mathbf{G_w}=\varepsilon_3=\begin{Bmatrix}\frac{\partial w}{\partial x} & \frac{\partial w}{\partial y}\end{Bmatrix}^T \tag{29}$$

By applying Eqs. (1)-(7) and (27)-(29), the matrices of in-plane forces for buckling solution based on finite strip method are expressed as:

$$\begin{Bmatrix}\varepsilon_1\\ \kappa_1\\ \chi_1\\ \chi_2\end{Bmatrix}=\sum_{m=1}^{r}\begin{Bmatrix}\mathbf{B}_m^{\mathbf{u}\varepsilon_1}\\ \mathbf{B}_m^{\mathbf{u}\kappa_1}\\ \mathbf{B}_m^{\chi_1}\\ \mathbf{B}_m^{\chi_2}\end{Bmatrix}\boldsymbol{\Delta}_m=\sum_{m=1}^{r}\mathbf{B}_m^{\mathbf{u}}\boldsymbol{\Delta}_m=\mathbf{B}^{\mathbf{u}}\boldsymbol{\Delta}; \tag{30}$$

$$\mathbf{B}^{\mathbf{u}}=[\mathbf{B}_1^{\mathbf{u}}\quad\mathbf{B}_2^{\mathbf{u}}\quad\dots\quad\mathbf{B}_r^{\mathbf{u}}]$$

$$\begin{Bmatrix}\varepsilon_2\\ \kappa_2\\ \chi_2\\ \chi_1\end{Bmatrix}=\sum_{m=1}^{r}\begin{Bmatrix}\mathbf{B}_m^{\mathbf{v}\varepsilon_2}\\ \mathbf{B}_m^{\mathbf{v}\kappa_2}\\ \mathbf{B}_m^{\chi_2}\\ \mathbf{B}_m^{\chi_1}\end{Bmatrix}\boldsymbol{\Delta}_m=\sum_{m=1}^{r}\mathbf{B}_m^{\mathbf{v}}\boldsymbol{\Delta}_m=\mathbf{B}^{\mathbf{v}}\boldsymbol{\Delta}; \tag{31}$$

$$\mathbf{B}^{\mathbf{v}}=[\mathbf{B}_1^{\mathbf{v}}\quad\mathbf{B}_2^{\mathbf{v}}\quad\dots\quad\mathbf{B}_r^{\mathbf{v}}]$$

$$\varepsilon_3 = \sum_{m=1}^{r} \mathbf{B}_m^{\mathbf{w}\varepsilon_3}\boldsymbol{\Delta}_m = \sum_{m=1}^{r} \mathbf{B}_m^{\mathbf{w}}\boldsymbol{\Delta}_m = \mathbf{B}^{\mathbf{w}}\boldsymbol{\Delta}; \quad \mathbf{B}^{\mathbf{w}} = [\mathbf{B}_1^{\mathbf{w}} \quad \mathbf{B}_2^{\mathbf{w}} \quad \dots \quad \mathbf{B}_r^{\mathbf{w}}] \tag{32}$$

where the matrices $\mathbf{B}_m^{\mathbf{u}\xi}$ for $\xi = \varepsilon_1, \kappa_1$, $\mathbf{B}_m^{\mathbf{v}\eta}$ for $\eta = \varepsilon_2, \kappa_2$, $\mathbf{B}_m^{\chi}$ for $\chi = \chi_1, \chi_2$ and $\mathbf{B}_m^{\mathbf{w}\varepsilon_3}$ are yield by applying the three matrices of each line as:

$$\mathbf{B}_m^{\mathbf{u}\xi} = \left[\mathbf{B}_{1m}^{\mathbf{u}\xi} \quad \mathbf{B}_{2m}^{\mathbf{u}\xi} \quad \mathbf{B}_{3m}^{\mathbf{b}\xi}\right]; (\xi = \varepsilon_1, \kappa_1) \tag{33}$$

$$\mathbf{B}_m^{\mathbf{v}\eta} = \left[\mathbf{B}_{1m}^{\mathbf{v}\eta} \quad \mathbf{B}_{2m}^{\mathbf{v}\eta} \quad \mathbf{B}_{3m}^{\mathbf{v}\eta}\right]; (\eta = \varepsilon_2, \kappa_2) \tag{34}$$

$$\mathbf{B}_m^{\chi} = \left[\mathbf{B}_{1m}^{\chi} \quad \mathbf{B}_{2m}^{\chi} \quad \mathbf{B}_{3m}^{\chi}\right]; (\chi = \chi_1, \chi_2) \tag{35}$$

$$\mathbf{B}_m^{\mathbf{w}\varepsilon_3} = \left[\mathbf{B}_{1m}^{\mathbf{w}\varepsilon_3} \quad \mathbf{B}_{2m}^{\mathbf{w}\varepsilon_3} \quad \mathbf{B}_{3m}^{\mathbf{w}\varepsilon_3}\right] \tag{36}$$

The matrices $\mathbf{B}_m^{\mathbf{u}\xi}$, $\mathbf{B}_m^{\mathbf{v}\eta}$, $\mathbf{B}_m^{\chi}$ and $\mathbf{B}_m^{\mathbf{w}\varepsilon_3}$ are written in Appendix B for different plate theories.

In Eq. (25), ρ_0 is the mass density of the laminate, $\overline{\rho}$ is a 2×2 matrix of the laminate density and $\mathbf{u}$ and w are the in–plane and out-of-plane displacements that defined in Eqs. (13) and (14). By applying Eqs. (1)-(7), (13) and (14), the $\mathbf{u}$ and w for free vibration solution based on finite strip method are rewritten as:

$$\begin{Bmatrix} \mathbf{u}_0 \\ \overline{\mathbf{w}} \\ \overline{\gamma} \end{Bmatrix} = \sum_{m=1}^{r} \begin{Bmatrix} \mathbf{B}_m^{\mathbf{mu}_0} \\ \mathbf{B}_m^{\mathbf{m}\overline{\mathbf{w}}} \\ \mathbf{B}_m^{\mathbf{m}\overline{\gamma}} \end{Bmatrix} \boldsymbol{\Delta}_m = \sum_{m=1}^{r} \mathbf{B}_m^{\mathbf{muv}}\boldsymbol{\Delta}_m = \mathbf{B}^{\mathbf{muv}}\boldsymbol{\Delta}; \quad \mathbf{B}^{\mathbf{muv}} = [\mathbf{B}_1^{\mathbf{muv}} \quad \mathbf{B}_2^{\mathbf{muv}} \quad \dots \quad \mathbf{B}_r^{\mathbf{muv}}] \tag{37}$$

$$w = \sum_{m=1}^{r} \mathbf{B}_m^{\mathbf{mw}}\boldsymbol{\Delta}_m = \mathbf{B}^{\mathbf{mw}}\boldsymbol{\Delta}; \quad \mathbf{B}^{\mathbf{mw}} = [\mathbf{B}_1^{\mathbf{mw}} \quad \mathbf{B}_2^{\mathbf{mw}} \quad \dots \quad \mathbf{B}_r^{\mathbf{mw}}] \tag{38}$$

where the matrix $\mathbf{B}_m^{\mathbf{m}\psi}$ is yield by applying three matrices for $\psi = u_0, \overline{w}, \overline{\gamma}$ and the three vectors for $\psi = w$ at each line as:

$$\mathbf{B}_m^{\mathbf{m}\psi} = \left[\mathbf{B}_{1m}^{\mathbf{m}\psi} \quad \mathbf{B}_{2m}^{\mathbf{m}\psi} \quad \mathbf{B}_{3m}^{\mathbf{m}\psi}\right]; (\psi = u_0, \overline{w}, \overline{\gamma}, w) \tag{39}$$

The matrix $\mathbf{B}_m^{\mathbf{m}\psi}$ is written in Appendix C for different plate theories. By applying Eqs. (18), (19), (30)-(32), (37) and (38), the Eq. (25) could be rewritten as:

$$\delta W_{int}^{b} + \delta W_{int}^{s} = \delta W_{ext}^{u} + \delta W_{ext}^{v} + \delta W_{ext}^{w} + \delta W_{ext}^{muv} + \delta W_{ext}^{mw} \tag{40}$$

where

$$\delta W_{int}^{\lambda_1} = \delta\boldsymbol{\Delta}^{\mathrm{T}}\left(\int_A \left(\mathbf{B}^{\lambda_1}\right)^{\mathrm{T}} \mathbf{D}_{\lambda_1}\mathbf{B}^{\lambda_1} dA\right)\boldsymbol{\Delta}; (\lambda_1 = b, s) \tag{41}$$

$$\delta W_{ext}^{\lambda_2} = \delta\boldsymbol{\Delta}^{\mathrm{T}}\left(\int_A \left(\mathbf{B}^{\lambda_2}\right)^{\mathrm{T}} \mathbf{S}_{\lambda_2}\mathbf{B}^{\lambda_2} dA\right)\boldsymbol{\Delta}; \quad (\lambda_2 = u, v, w) \tag{42}$$

$$\delta W_{ext}^{\lambda_3} = \delta\boldsymbol{\Delta}^{\mathrm{T}}\left(\int_A \left(\mathbf{B}^{\lambda_3}\right)^{\mathrm{T}} \mathbf{I}_{\lambda_3}\mathbf{B}^{\lambda_3} dA\right)\boldsymbol{\Delta}; \quad (\lambda_3 = muv, mw) \tag{43}$$

where A is the strip area. The virtual work is valid for any variation of $\delta\boldsymbol{\Delta}^{\mathrm{T}}$, hence, the FE formulation can be expressed in a matrix form as:

$$\left(\mathbf{K} - N_{cr}\mathbf{K_g}\right)\boldsymbol{\Delta} = \mathbf{0}; \quad (\mathbf{K} - \omega_{cr}^2\mathbf{M})\boldsymbol{\Delta} = \mathbf{0} \tag{44}$$

in which N_{cr} and ω_{cr} are the critical load of the laminate and the natural frequency, respectively. The stiffness matrix $\mathbf{K}$, geometric matrix $\mathbf{K}_g$ and mass matrix $\mathbf{M}$ are expressed as:

$$\mathbf{K} = \int_A \left(\mathbf{B^b}\right)^{\mathrm{T}}\mathbf{D_b}\mathbf{B^b}dA + \int_A (\mathbf{B^s})^{\mathrm{T}}\mathbf{D_s}\mathbf{B^s}dA \tag{45}$$

$$\mathbf{K_g} = \int_A (\mathbf{B^u})^{\mathrm{T}}\mathbf{S_u}\mathbf{B^u}dA + \int_A (\mathbf{B^v})^{\mathrm{T}}\mathbf{S_v}\mathbf{B^v}dA + \int_A (\mathbf{B^w})^{\mathrm{T}}\mathbf{S_w}\mathbf{B^w}dA \tag{46}$$

$$\mathbf{M} = \int_A (\mathbf{B^{muv}})^{\mathrm{T}}\mathbf{I_{muv}}\mathbf{B^{muv}}dA + \int_A (\mathbf{B^{mw}})^{\mathrm{T}}\mathbf{I_{mw}}\mathbf{B^{mw}}dA \tag{47}$$

The matrices $\mathbf{D_b}$, $\mathbf{D_s}$, $\mathbf{S_u}$, $\mathbf{S_v}$, $\mathbf{S_w}$, $\mathbf{I_{muv}}$ and $\mathbf{I}_{mw}$ are written in Appendices D to F for different plate theories.

3. Numerical study

The different numerical examples are presented for buckling and free vibration analysis of isotropic and laminated composites plates with cross-ply and angle-ply laminations based on different plate theories subjected to different length to thickness ratio, lamination angles, and boundary conditions. Each longitudinal finite strip consists of $20r$ DOF for RPT theory and $22r$ DOF for other theories such as Zigzag and higher order theories, where, r is the number of modes. In all tables and figures, a, b and h represent the plate width, length, and thickness, respectively. The material properties $E = 200$ GPa, $\nu = 0.3$ for an isotropic plates and $G_{12} = G_{13} = 0.6E_2, G_{23} = 0.6E_2, \nu_{12} = 0.25$ for laminated plates.

Non–dimensional buckling load and natural frequency for the isotropic plate are expressed by the following equations:

$$k = \frac{N_{cr}a^2}{\pi^2 D}; \quad \widehat{\omega} = \frac{\omega_{cr}a^2}{\pi^2}\sqrt{\frac{\rho_0 h}{D}} \quad \widetilde{\omega} = \frac{\omega_{cr}a^2}{h}\sqrt{\frac{\rho_0}{E}} \tag{48}$$

where $D = \frac{Eh^3}{12(1-\nu^2)}$.

Non–dimensional buckling load and natural frequency for an orthotropic plate can be expressed as follows:

$$\overline{N} = \frac{N_{cr}a^2}{E_2 h^3}; \quad \overline{\omega} = \omega_{cr}a^2\sqrt{\frac{\rho_0}{E_2 h^2}} \tag{49}$$

Table 2 Different boundary conditions for different theories and ply orientation

Theories	Laminate	Boundary conditions at $x=0,b$ Simply Supported (S)	Clamped (C)	Free (F)
RPT	cross-ply	$v=\bar{v}=w_b=w_s=0$	$u=\bar{u}=v=\bar{v}=w_b=0$ $\frac{\partial w_b}{\partial x}=w_s=\frac{\partial w_s}{\partial x}=0$	All DOFs are released
	angle-ply	$u=\bar{u}=w_b=w_s=0$	$u=\bar{u}=v=\bar{v}=w_b=0$ $\frac{\partial w_b}{\partial x}=w_s=\frac{\partial w_s}{\partial x}=0$	All DOFs are released
Others	cross-ply	$v=\bar{v}=w=\gamma_y=0$	$u=\bar{u}=v=\bar{v}=0$ $\frac{\partial w}{\partial x}=w=\gamma_x=\gamma_y=0$	All DOFs are released
	angle-ply	$u=\bar{u}=w=\gamma_y=0$	$u=\bar{u}=v=\bar{v}=0$ $\frac{\partial w}{\partial x}=w=\gamma_x=\gamma_y=0$	All DOFs are released

Table 3 The effect of the number of strips on non-dimensional critical uniaxial buckling load of isotropic square plate based on TSDT theory, (Kg-w)

Number of Strips	a/h=2	a/h=4	a/h=5	a/h=10	a/h=20	a/h=50
1	1.7259	3.1040	3.4386	4.0183	4.1956	4.2482
2	1.6784	2.9655	3.2710	3.7942	3.9528	3.9996
5	1.6760	2.9609	3.2655	3.7868	3.9446	3.9912
10	1.6760	2.9607	3.2654	3.7866	3.9444	3.9910
20	1.6760	2.9607	3.2653	3.7866	3.9444	3.9910
100	1.6760	2.9607	3.2653	3.7866	3.9444	3.9910
Zenkour (2004)	1.6760	2.9607	3.2653	3.7866	3.9444	3.9910

Table 4 The non–dimensional critical buckling load (k) of simply supported isotropic square plate with $n_y=1$, (Kg-w)

		FSDT of Mindlin		HSDT of Touratier		TSDT of Reddy	
n_x	a/h	Present	Zenkour (2004)	Present	Zenkour (2004)	Present	Zenkour (2004)
0	2	1.6598	1.6598	1.6811	1.6811	1.6760	1.6760
	4	2.9575	2.9575	2.9626	2.9626	2.9607	2.9607
	5	3.2637	3.2637	3.2666	3.2666	3.2654	3.2653
	10	3.7865	3.7865	3.7869	3.7869	3.7866	3.7866
	20	3.9444	3.9444	3.9445	3.9445	3.9444	3.9444
	50	3.9910	3.9910	3.9910	3.9910	3.9910	3.9910
0.5	2	1.1065	1.1065	1.1207	1.1207	1.1173	1.1173
	4	1.9719	1.9717	1.9751	1.9751	1.9738	1.9738
	5	2.1758	2.1758	2.1777	2.1777	2.1769	2.1769
	10	2.5243	2.5243	2.5246	2.5246	2.5244	2.5244
	20	2.6296	2.6296	2.6297	2.6297	2.6296	2.6296
	50	2.6607	2.6607	2.6607	2.6608	2.6607	2.6607
1	2	0.8299	0.8299	0.8405	0.8405	0.8380	0.8380
	4	1.4788	1.4788	1.4813	1.4813	1.4804	1.4804
	5	1.6319	1.6319	1.6333	1.6333	1.6327	1.6327
	10	1.8932	1.8932	1.8935	1.8935	1.8933	1.8933
	20	1.9722	1.9722	1.9722	1.9722	1.9722	1.9722
	50	1.9955	1.9955	1.9955	1.9955	1.9955	1.9955

In the finite strip method, the two opposite edges in the longitudinal direction are assumed to be simply supported, while, the other two edges in the transverse direction can have arbitrary boundary conditions. The mechanical boundary conditions for different boundary conditions and different orientation of plies are tabulated in Table 2.

3.1 Critical loads of the isotropic plates

For verification and accuracy, the non-dimensional critical uniaxial buckling load of simply supported isotropic square plate with different length to thickness ratios based on TSDT are tabulated in Table 3. The results are obtained with a different number of strips based on the one mode. It

Table 5 The non–dimensional uniaxial critical buckling load (k) of simply supported isotropic rectangular plate according to TSDT of Reddy, (Kg-w)

	$a/b = 0.2$		$a/b = 0.4$		$a/b = 0.8$		$a/b = 1.0$	
a/h	Present	Reddy (2004)	Present	Reddy (2004)	Present	Reddy (2004)	Present	Reddy (2004)
2	1.6852	1.6851	1.4455	1.4455	1.5180	1.5179	1.6760	1.6759
5	7.0532	7.0529	4.6467	4.6466	3.2627	3.2626	3.2654	3.2653
10	15.6589	15.658	6.9854	6.9853	3.9195	3.9195	3.7866	3.7865
20	22.8594	22.859	8.0014	8.0010	4.1280	4.1279	3.9444	3.9443
50	26.2702	26.270	8.3419	8.3417	4.1904	4.1903	3.9910	3.9909
100	26.8435	26.843	8.3929	8.3928	4.1995	4.1994	3.9978	3.9977

Table 6 The non-dimensional uniaxial critical buckling load (k) of isotropic square plate for different boundary conditions in the transverse direction, (Kg-w)

		Boundary conditions					
h/a	Methods	SS	CC	CS	CF	SF	FF
0.001	RPT of Shimpi	4.0000	7.6920[a]	5.7403	1.6525	1.4016	0.9523
	TSDT of Reddy	4.0000	7.6920[a]	5.7403	1.6525	1.4016	0.9523
	Zenkour (2004)	4.000	7.691	5.740	1.663	1.402	0.9523
	Hosseini *et al.* (2008)	4.000	7.6911	5.7401	1.6522	1.4014	0.95225
0.05	RPT of Shimpi	3.9444	7.3778[a]	5.6298	1.6377	1.3907	0.9460
	TSDT of Reddy	3.9444	7.3192[a]	5.6038	1.6231	1.3832	0.9438
	Zenkour (2004)	3.944	7.299	5.574	1.620	1.378	0.9412
	Hosseini *et al.* (2008)	3.9437	7.2989	5.5977	1.6197	1.3813	0.94314
0.1	RPT of Shimpi	3.7866	6.5731[a]	5.3225	1.5949	1.3589	0.9274
	TSDT of Reddy	3.7866	6.4231[a]	5.2375	1.5592	1.3422	0.9225
	Zenkour (2004)	3.784	6.370	5.140	1.556	1.327	0.9146
	Hosseini *et al.* (2008)	3.7838	6.3698	5.2171	1.5558	1.3707	0.92187
0.2	RPT of Shimpi	3.2654	4.5863[a]	4.2631[a]	1.4438	1.2452	0.8602
	TSDT of Reddy	3.2654	4.4135[a]	4.2631[a]	1.3769	1.2163	0.8515
	Zenkour (2004)	3.256	4.320	3.876	1.370	1.173	0.8274
	Hosseini *et al.* (2008)	3.2558	4.3204	4.1364	1.3701	1.2138	0.85011

[a] $r = 2$

can be deduced that an increase in the number of strips is effective when it reaches ten, while after ten, no effect is observed. Therefore, in the context, the applied ten strips and one mode $(r = 1)$ prevail unless other value is stipulated in the process. In addition, it shows that compared to other numerical methods, it is possible to achieve more accurate results with fewer degrees of freedom. From now on the 'Kg-w' reveals that in Eq. (46) the only third term is applied for calculating the geometric stiffness $\mathbf{K_g}$, while 'Kg-uvw' reveals that all three terms are applied.

The isotropic square plate with the given material and simply supported boundary condition on four edges subjected to in-plane forces in one and two directions and the outcomes are tabulated in Table 4, the obtained results indicate an excellent agreement with Reddy (2004). The non-dimensional buckling load of the isotropic simply supported rectangular plate with $a/b = 0.2, 0.4, 0.8$ and 1, is tabulated in Table 5. The results obtained based on TSDT are of good convergence and accuracy with Reddy (2004). The results of the isotropic square plate with different boundary conditions in the transverse direction with $h/a = 0.001, 0.05, 0.1$ and 0.2 for two plate theories, RPT of Shimpi and TSDT of Reddy are tabulated in Table 6, where, a good agreement is observed with the exact solution and spline finite strip solution.

3.2 Critical loads of cross-ply and angle-ply laminated plates

The uniaxial critical buckling loads of symmetric cross-ply laminated square plate is subjected to compressive load in y direction, with different length to thickness ratios and modulus ratios, Table 7. This plate which is composed of four equally thick layers oriented at $[0/90]_s$ is simply supported on all the edges. The results are obtained through this finite strip method based on three theories CLPT, FSDT and TSDT are in good agreement with those in Reddy (2004).

In Table 8, a simply supported symmetric cross-ply $[0/90]_s$ laminated square plate subjected to uniaxial compressive load with different modulus ratios is of concern. where, the results are presented for TSDT, Zigzag theory and RPT with length to thickness ratios $a/h = 5{,}10$. It is observed that the results are presented for the non-dimensional uniaxial critical buckling load based on TSDT and Zigzag theories are close. Despite the increase in modulus ratio, the difference between the results of these

Table 7 The non-dimensional uniaxial critical buckling load ($\overline{N}$) of simply supported cross-ply laminated square plate $[0/90]_s$, (Kg-w)

		CLPT		FSDT		TSDT of Reddy	
a/h	E_1/E_2	Present	Reddy (2004)	Present	Reddy (2004)	Present	Reddy (2004)
10	3	5.7538	5.754	5.3991	5.399	5.3933	5.393
10	10	11.4919	11.492	9.9654	9.965	9.9406	9.941
10	20	19.7126	19.712	15.3515	15.351	15.2985	15.298
10	30	27.9360	27.936	19.7568	19.756	19.6745	19.674
5	40	36.1601	36.160	12.1462	11.575	11.9972	11.997
10	40	36.1601	36.160	23.4530	23.453	23.3402	23.340
20	40	36.1601	36.160	31.7073	31.707	31.6599	31.660
50	40	36.1601	36.160	35.3564	35.356	35.3471	35.347
100	40	36.1601	36.160	35.9554	35.955	35.9530	35.953

Table 8 The effect of modulus ratio on the non-dimensional uniaxial critical buckling load of simply supported cross-ply laminated square plate $[0/90]_s$, (Kg-uvw)

	$a/h=5$			$a/h=10$		
E_1/E_2	TSDT of Reddy	Zigzag of Cho	RPT of Shimpi	TSDT of Reddy	Zigzag of Cho	RPT of Shimpi
3	4.3598	4.3596	4.4140	5.3159	5.3157	5.3364
10	6.9327	6.9451	7.4470	9.8125	9.8171	10.0821
20	9.1949	9.2318	10.4417	15.1253	15.1423	16.0515
30	10.6905	10.7549	12.5135	19.4749	19.5087	21.2228
40	11.7903	11.8833	14.0387	23.1246	23.1785	25.7459

two theories is not significant, while, the difference between the non-dimensional uniaxial critical buckling for RPT theory increases as compared with the two other theories when modulus ratio is increased from 3 to 40.

The critical outputs of the buckling load of cross-ply laminated square plate $[0/90]_n$ with 2 and 10 layers ($n=1,5$), different length to thickness ratios and different boundary conditions based on HSDT of Touratier, HSDT of Afaq and TSDT of Reddy are tabulated in Table 9. The same procedure is followed for the laminated square plate $[(0/90)_n/0]$ with 2, 5 and 9 layers ($n=1,2,4$), Table 10 and for $[0/90/0]$, Table 11 based on different plate theories.

The non-dimensional buckling load of antisymmetric angle-ply laminated square plate $[\theta/-\theta]_n$ with 2 and 6 layers ($n=1,3$) with different length to thickness ratios for three angles $\theta=5°, 30°$ and $45°$ based on TSDT of the Reddy theory are tabulated in Table 12, where a good agreement is observed with Reddy (2004).

The effect of the number of layers on the non-dimensional uniaxial critical buckling load of simply supported cross-ply laminated square plate $[0/90]_n$ with ($n=1,2,3,4,5$) is diagrammed in Fig. 2 at modulus ratio $E_1/E_2=40$ based on TSDT. It is observed that regardless of the effect of the number of layers, an increase in the length to thickness ratios beginning from $a/h=20$, whould increase the non-dimensional buckling load, after which no significant change is observed. An increase in the number of layers significantly increase the non-dimensional buckling load from 2 to 4 layers, while, an increase more than these layers, no considerable change is observed in this parameter.

3.3 Interaction curves of critical biaxial in-plane loading

The effect of boundary conditions on the non-dimensional critical biaxial buckling load of cross-ply laminated square plate $[0/90/0]$ with modulus ratio $E_1/E_2=40$ and length to thickness ratio $a/h=10$ are diagrammed based on TSDT, Fig. 3(a). The interaction curves indicate that for plate with fixed and simply supported boundary conditions on the edges ($x=0,a$), the non–dimensional critical buckling load varies linearly, while, for a plate of at least one free boundary condition on the edges ($x=0$ or $x=a$), this parameter varies nonlinearly.

The effect of modulus ratio on the non-dimensional critical biaxial buckling load of simply supported cross-ply laminated square plate $[0/90/90/0]$ with length to thickness ratio $a/h=10$ based on TSDT is diagrammed in Fig. 3(b). Here, it is observed that the non-dimensional critical buckling loads increase by an increase in the modulus ratio and the interaction curves are linear. The interaction curves of the non-dimensional critical biaxial buckling loads of simply supported angle-ply laminated square plate $[\theta/-\theta]$ with different lamination angle are diagrammed in Fig. 3(c). The same curves for laminate $[30/-30]_n$ with the different, the number of layers ($n=1,2,3,4,5$) are diagrammed in Fig. 3(d).

Table 9 The non–dimensional uniaxial critical buckling load $(\overline{N})$ of cross-ply laminated square plate $[0/90]_n$ with modulus ratio $E_1/E_2 = 40$ for different boundary conditions in the transverse direction, (Kg-uvw)

			Boundary Conditions					
n	a/h	Theory	FF	FS	FC	SS	SC[a]	CC[a]
1	5	HSDT of Touratier	3.8351	4.1616	4.7652	8.4340	10.5755	11.4149
		HSDT of Afaq	3.8708	4.1985	4.8081	8.5128	10.8307	11.7166
		TSDT of Reddy	3.8043	4.1299	4.7282	8.3667	10.3557	11.1544
		TSDT of Reddy (Kg-w)	3.9055	4.2855	4.9132	8.7695	10.7555	11.4989
		Reddy (2004)-Levy	3.905	4.283	4.908	8.769	10.754	11.490
		Reddy (2004)-FEM	3.979	4.375	5.022	8.985	11.241	12.318
	10	HSDT of Touratier	4.8971	5.3790	6.1976	11.3440	16.8871	20.9980
		HSDT of Afaq	4.9109	5.3936	6.2147	11.3768	16.9860	21.2089
		TSDT of Reddy	4.8852	5.3665	6.1828	11.3159	16.8014	20.8157
		TSDT of Reddy (Kg-w)	4.9400	5.4453	6.2810	11.5626	17.1526	21.4899
		Reddy (2004)-Levy	4.940	5.442	6.274	11.562	17.133	21.464
		Reddy (2004)-FEM	5.090	5.621	6.487	12.011	18.257	24.262
5	5	HSDT of Touratier	6.7565	6.9682	8.1597	13.8447	12.6603	13.3789
		HSDT of Afaq	6.7883	7.0008	8.2004	13.9131	12.8707	13.6290
		TSDT of Reddy	6.7389	6.9501	8.1353	13.8060	12.5011	13.1857
		TSDT of Reddy (Kg-w)	6.7799	7.0531	8.2252	13.9631	12.6111	13.2635
		Reddy (2004)-Levy	6.780	7.050	8.221	12.109	12.607	13.254
		Reddy (2004)-FEM	6.802	7.089	8.278	12.224	12.800	13.659
	10	HSDT of Touratier	12.0274	12.4287	14.2633	25.2105	32.7003	35.2920
		HSDT of Afaq	12.0429	12.4448	14.2825	25.2453	32.8588	35.4925
		TSDT of Reddy	12.0220	12.4230	14.2558	25.1981	32.6088	35.1684
		TSDT of Reddy (Kg-w)	12.0774	12.5096	14.3586	25.4226	32.9026	35.4290
		Reddy (2004)-Levy	12.077	12.506	14.351	25.423	32.885	35.376
		Reddy (2004)-FEM	12.248	12.699	14.568	25.828	33.662	36.657

Table 10 The non-dimensional uniaxial critical buckling load $(\overline{N})$ of simply supported cross-ply laminated square plate $[(0/90)_n/0]$ with length to thickness ratio $a/h = 10$, (Kg-uvw)

		E_1/E_2				
n	Theory	3	10	20	30	40
1	Zigzag of Cho	5.3109	9.7029	14.7167	18.6819	21.9148
	TSDT of Reddy	5.3124	9.7047	14.7169	18.6772	21.9019
	TSDT of Reddy (Kg-w)	5.3899	9.8326	14.8897	18.8777	22.1209
	Zenkour (2004)	5.3899	9.8325	14.8896	18.8776	22.1207
	Yang and He (2018)	5.3880	9.8255	14.8702	18.8412	22.0635
	Singh and Singh (2017)-TDT	5.4002	9.8771	14.9984	17.8442	20.2231
	Singh and Singh (2017)-THDT	5.4121	9.9115	15.0016	17.6452	20.8743
2	Zigzag of Cho	5.3255	9.9423	15.5628	20.2886	24.3306
	TSDT of Reddy	5.3290	9.9596	15.6107	20.3739	24.4563
	TSDT of Reddy (Kg-w)	5.4067	10.0897	15.7880	20.5782	24.6757
	Zenkour (2004)	5.4066	10.0897	15.7879	20.5781	24.6755
	Yang and He (2018)	5.3968	10.0213	15.5987	20.2419	24.2772
	Singh and Singh (2017)-TDT	5.4174	10.1168	15.8449	20.6700	24.8053
	Singh and Singh (2017)-THDT	5.4280	10.2108	16.0410	20.9958	25.4594
4	Zigzag of Cho	5.3313	10.0332	15.8864	20.9089	25.2703
	TSDT of Reddy	5.3343	10.0464	15.9221	20.9727	25.3652
	TSDT of Reddy (Kg-w)	5.4120	10.1773	16.1009	21.1784	25.5846
	Zenkour (2004)	5.4120	10.1772	16.1009	21.1783	25.5845
	Yang and He (2018)	5.4226	10.2045	16.1602	21.2753	25.7218
	Singh and Singh (2017)-TDT	5.4417	10.2087	16.2580	21.5299	26.2531

Table 11 The non-dimensional biaxial critical buckling load $(\bar{N})$ of simply supported cross-ply laminated square plate $[0/90/0]$ with length to thickness ratio $a/h = 10$, (Kg-uvw)

	$a/h = 10$				$E_1/E_2 = 40$				
	E_1/E_2				a/h				
Theory	10	20	30[a]	40[a]	2[a]	5[a]	10[a]	15[a]	20[a]
FSDT of Mindlin	4.8712	7.4049	8.7387	9.9491	1.3725	5.3637	9.9491	12.0198	13.0315
TSDT of Reddy	4.8524	7.3568	8.5902	9.7311	1.4158	5.2331	9.7311	11.8816	12.9407
HSDT of Touratier	4.8514	7.3568	8.5720	9.7041	1.4169	1.8646	9.7041	12.296	12.9296
HSDT of Afaq	4.8526	7.3606	8.5591	9.6839	1.4237	5.1754	9.6839	11.8524	12.9218
Zigzag of Cho	4.8515	7.3583	8.6384	9.8056	1.4828	5.3575	9.8056	11.9226	12.9656
Tran et al. (2014)-ITSDT	4.9130	7.4408	8.775	9.8795	1.4316	5.3236	9.8795	11.9978	13.0239
Tran et al. (2014)-layerwise	4.9707	7.5665	8.8772	10.0033	1.5015	5.4586	10.0033	12.0907	13.0892

[a] $r=2$

Table 12 The non-dimensional uniaxial critical buckling load $(\bar{N})$ of simply supported antisymmetric angle-ply laminated square plate $[\theta/-\theta]_n$ $(n = 1,3)$ with modulus ratio $E_1/E_2 = 40$, (Kg-uvw)

		$\theta = 5°$		$\theta = 30°$		$\theta = 45°$	
a/h	Theory	$n = 1$	$n = 3$	$n = 1$	$n = 3$	$n = 1$	$n = 3$
5	TSDT of Reddy	10.3135	10.7769	11.1611	9.3058[a]	10.4905[a]	12.1016[a]
	Reddy (2004)	10.674	11.082	11.547	13.546	10.881	12.169
10	TSDT of Reddy	20.5183	22.3385	16.7905	33.4530	17.8234	32.0957[a]
	Reddy (2004)	20.989	22.592	17.127	33.701	18.154	32.405
20	TSDT of Reddy	28.1077	31.4545	19.4324	47.4819	20.5640	53.0260
	Reddy (2004)	28.308	31.577	19.561	47.643	20.691	53.198
50	TSDT of Reddy	31.5196	35.6317	20.3556	53.9142	21.5160	60.7197
	Reddy (2004)	31.519	35.657	20.379	53.951	21.539	60.760

[a] $r=2$

Table 13 The non-dimensional natural frequency $\tilde{\omega}$ of isotropic square plate with different length to thickness ratios for $\nu = 0.34$, based on different plate theories

	a/h				
Theory	4	10	20	50	100
FSDT of Mindlin	5.0316	5.8431	6.0024	6.0500	6.0569
TSDT of Reddy	5.0342	5.8432	6.0024	6.0500	6.0569
HSDT of Touratier	5.0356	5.8434	6.0025	6.0500	6.0569
HSDT of Afaq	5.0390	5.8442	6.0027	6.0500	6.0569
RPT of Shimpi	5.0342	5.8432	6.0024	6.0500	6.0569
RPT of Reddy	5.0342	5.8432	6.0024	6.0500	6.0569
RPT of Touratier	5.0356	5.8434	6.0025	6.0500	6.0569
RPT of Mechab	5.0341	5.8432	6.0024	6.0500	6.0569
Zigzag of Cho	5.0342	5.8432	6.0024	6.0500	6.0569

As shown in Fig. 3(c), the maximum buckling load in biaxial loading occurs at $\theta = 0°$ and an increase in the angle of laminate up to $\theta = 30°$, the buckling load decreases. Following this, an increase in θ increases the non-dimensional buckling load . In Fig. 3(d) an increase in the number of layers from 2 to 4, increases the non-dimensional buckling load significantly, while, more than four layers, no considerable change is observed.

3.4 Natural frequency of the isotropic plates

Here, in all cases, $\rho_0 = 1$ is the mass density per unit of volume. The effects of length to thickness ratios of the plate and different plate theories are assessed on the non-dimensional fundamental frequency with Poisson's ratio $\nu = 0.34$ on simply supported isotropic square plate are tabulated in Table 13. As observed the results are obtained through this proposed method and are in good agreement with other references.

Table 14 The non-dimensional natural frequency $\widehat{\omega}$ of isotropic square plate with different length to thickness ratios and different boundary conditions in the longitudinal direction based on different plate theories

		CLPT	FSDT	HSDT			RPT			Zigzag
a/h	BCs	Kirchhoff	Mindlin	Reddy	Touratier	Afaq	Shimpi	Reddy	Touratier	Cho
5	SS	1.9373	1.7679	1.7683	1.7686	1.7694	1.7683	1.7683	1.7683	1.7683
	CC	2.8317	2.2832	2.2902	2.2922	2.2955	2.3836	2.3836	2.3849	2.2902
	SC	2.3159	2.0028	2.0056	2.0066	2.0083	2.0489	2.0489	2.0495	2.0056
	SF	1.1594	1.0840	1.0842	1.0844	1.0847	1.0975	1.0975	1.0976	1.0842
	CF	1.2572	1.1523	1.1529	1.1531	1.1536	1.1812	1.1812	1.1813	1.1529
	FF	0.9600	0.9102	0.9103	0.9104	0.9106	0.9150	0.9150	0.9151	0.9103
10	SS	1.9838	1.9317	1.9317	1.9318	1.9320	1.9317	1.9317	1.9318	1.9317
	CC	2.9070	2.7105	2.7114	2.7119	2.7129	2.7560	2.7560	2.7563	2.7114
	SC	2.3751	2.2712	2.2715	2.2717	2.2722	2.2898	2.2898	2.2900	2.2715
	SF	1.1776	1.1527	1.1527	1.1528	1.1529	1.1599	1.1599	1.1599	1.1527
	CF	1.2783	1.2419	1.2421	1.2421	1.2423	1.2562	1.2562	1.2563	1.2421
	FF	0.9718	0.9566	0.9567	0.9567	0.9568	0.9593	0.9593	0.9593	0.9567
20	SS	1.9959	1.9821	1.9821	1.9821	1.9822	1.9821	1.9821	1.9821	1.9821
	CC	2.9268	2.8713	2.8714	2.8715	2.8718	2.8853	2.8853	2.8854	2.8714
	SC	2.3907	2.3622	2.3623	2.3623	2.3624	2.3677	2.3677	2.3678	2.3623
	SF	1.1823	1.1745	1.1746	1.1746	1.1746	1.1777	1.1777	1.1777	1.1746
	CF	1.2837	1.2722	1.2722	1.2723	1.2723	1.2780	1.2780	1.2780	1.2722
	FF	0.9748	0.9705	0.9705	0.9705	0.9705	0.9716	0.9716	0.9716	0.9705
50	SS	1.9993	1.9971	1.9971	1.9971	1.9971	1.9971	1.9971	1.9971	1.9971
	CC	2.9324	2.9231	2.9231	2.9232	2.9232	2.9255	2.9255	2.9256	2.9231
	SC	2.3951	2.3904	2.3904	2.3904	2.3904	2.3913	2.3913	2.3913	2.3904
	SF	1.1836	1.1822	1.1822	1.1822	1.1822	1.1829	1.1829	1.1829	1.1822
	CF	1.2852	1.2830	1.2830	1.2830	1.2830	1.2843	1.2843	1.2843	1.2830
	FF	0.9757	0.9749	0.9749	0.9749	0.9749	0.9752	0.9752	1.2843	0.9749

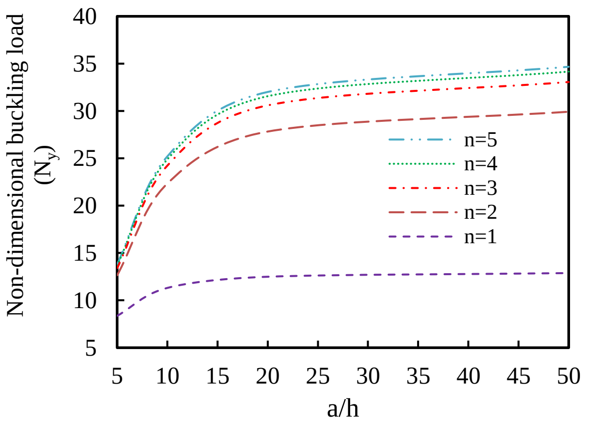

Fig. 2 The effect of the number of layers on the non-dimensional uniaxial critical buckling load $(\overline{N})$ of simply supported cross-ply laminated square plate $[0/90]_n$ with $(n = 1,2,3,4,5)$ at $E_1/E_2 = 40$ based on TSDT

The non-dimensional fundamental frequency for different boundary conditions and length to thickness ratios obtained through different plate theories tabulated in Table 1 are tabulated in Table 14. In this table, based on CLPT, a change in length to thickness ratio, changes the non-dimensional fundamental frequency due to Eq. (47), where in-plane displacement fields are applied to calculate the Mass matrix.

3.5 The Natural frequency of the cross-ply and the angle-ply laminated plates

The non-dimensional natural frequency of simply supported cross-ply laminated square plate $[0/90]_s$, $[0/90]$ and $[0/90]_n$ with different length to thickness ratios, different modulus ratios and boundary conditions based on different plate theories with different modulus ratios are calculated through this proposed formulation and the results are tabulated in Tables 15 to 17.

As observed in Tables 15 to 17, the obtained results for the non-dimensional natural frequency based on the aforementioned plate theories where the finite strip formulation are applied, are in a good agreement with other references. As observed in Table 16 the results of the four symmetric cross-ply laminated plate based on RPT of Shimpi theory are closer than the other two theories, as to the two layers antisymmetric cross-ply laminated plate the results are close together. Here, it can be deduced that, although RPT theory is of high accuracy for antisymmetric cross-ply laminated plates, the same does not hold true for symmetric cross-ply laminated plates, Table 17.

The non-dimensional natural frequency of simply supported angle-ply laminated square plate $[\theta/-\theta]_n$ with $n = 1,3,4$ and $[45/-45/45]$ at modulus ratio $E_1/E_2 = 40$ based on TSDT of Reddy, HSDT of Touratier and Zigzag of Cho are tabulated in Tables 18 and 19, respectively. The results tabulated here, indicate that non-dimensional natural frequency increases by an increase

Table 15 The non-dimensional natural frequency ($\overline{\omega}$) of simply supported cross-ply laminated square plate $[0/90]_s$ based on different HSDT plate theories

E_1/E_2	a/h	Present Study			Reddy (2004)	Tran *et al.* (2014)	Fallah and Delzendeh (2018)
		HSDT of Touratier	HSDT of Afaq	TSDT of Reddy	HSDT of Reddy	HSDT	FSDT
3	5	6.5601	6.5626	6.5597	6.5597	—	—
	10	7.2434	7.2442	7.2433	7.2433	—	—
10	5	8.2737	8.2806	8.2718	8.2718	8.2944	8.3072
	10	9.8417	9.8447	9.841	9.841	—	—
20	5	9.5302	9.5421	9.5263	9.5263	9.5650	9.6086
	10	12.2205	12.2275	12.2181	12.2181	—	—
30	5	10.2769	10.2921	10.2719	10.2719	10.3206	10.3436
	10	13.8681	13.8791	13.8639	13.8639	—	—
40	5	10.7938	10.8105	10.7873	10.7873	10.8428	10.8532
	10	15.1130	15.1276	15.1073	15.1073	15.1552	—

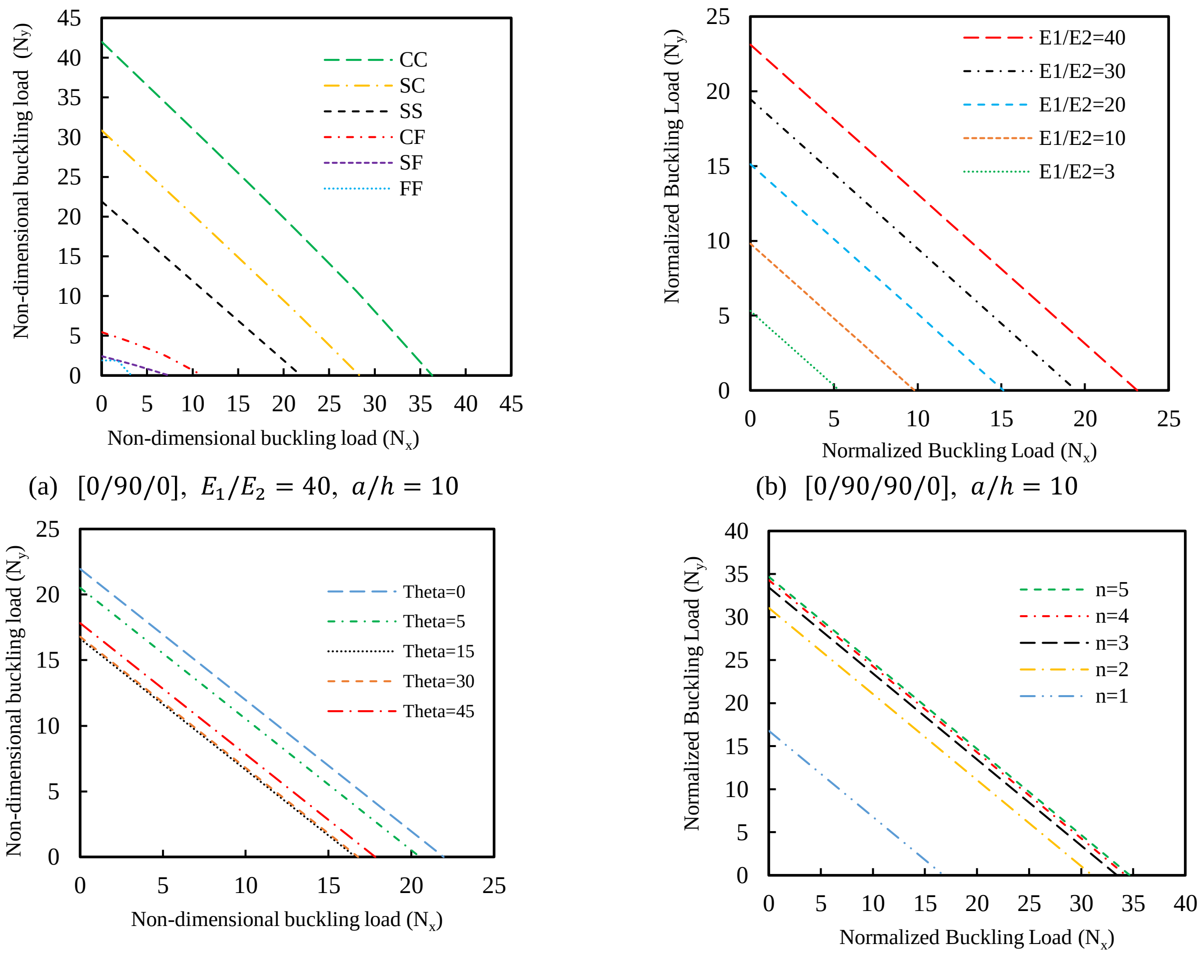

(a) $[0/90/0]$, $E_1/E_2 = 40$, $a/h = 10$

(b) $[0/90/90/0]$, $a/h = 10$

(c) $[\theta/-\theta]$, $E_1/E_2 = 40$, $a/h = 10$

(d) $[30/-30]_n$, $E_1/E_2 = 40$, $a/h = 10$

Fig. 3 Interaction curves of biaxial in-plane loading on the non-dimensional buckling load ($\overline{N}$) of simply supported cross-ply and angle-ply laminated square plate based on TSDT

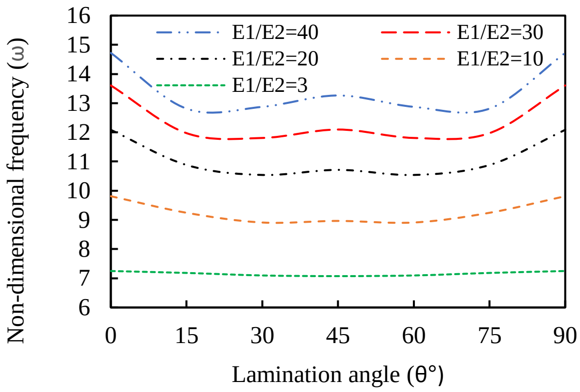

$(a)\ a/h = 10$

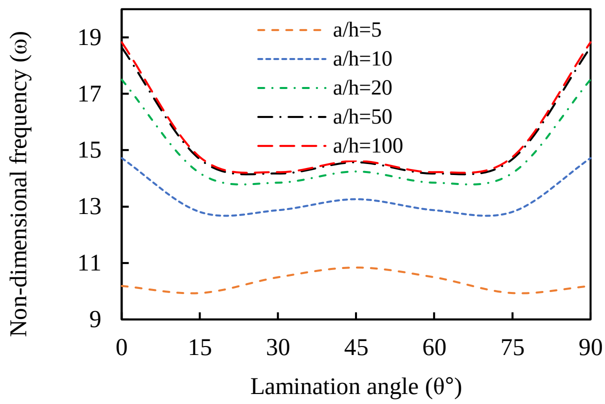

$(b)\ E_1/E_2 = 40$

Fig. 4 The effect of lamination angle on the non-dimensional natural frequency $(\overline{\omega})$ of simply supported angle-ply laminated square plate $[\theta/-\theta]$ based on TSDT

Table 16 The non-dimensional natural frequency $(\overline{\omega})$ of simply supported cross-ply laminated square plate with modulus ratio $E_1/E_2 = 40$

	[0/90]				[0/90/90/0]			
	Present Study			Bouazza et al. (2017)	Present Study			Bouazza et al. (2017)
a/h	TSDT of Reddy	Zigzag of Cho	RPT of Shimpi	RPT	TSDT of Reddy	Zigzag of Cho	RPT of Shimpi	RPT
5	9.0871	9.1866	9.0871	9.0871	10.7873	10.8298	11.7710	11.1802
10	10.568	10.606	10.5680	10.568	15.1073	15.1249	15.9406	15.979
12.5	10.8135	10.8395	10.8135	10.8135	16.1603	16.1727	16.8289	16.860
20	11.1052	11.1161	11.1052	11.1052	17.6466	17.6522	17.9939	18.010
25	11.1768	11.1840	11.1768	11.1768	18.062	18.0657	18.3012	18.312
50	11.2751	11.2769	11.2751	11.2751	18.6719	18.6729	18.7382	18.741
100	11.3002	11.3006	11.3002	11.3002	18.8357	18.8360	18.8527	18.853

Table 17 The non-dimensional natural frequency $(\overline{\omega})$ of simply supported laminated square plate $[0/90]_n$ based on different theories and different boundary conditions in the transverse direction

			Boundary Conditions					
n	a/h	Theory	FF	FS	FC	SS	SC	CC
1	5	Zigzag of Cho	6.1991	6.4536	6.9042	9.1866	10.5722	12.1701
		RPT of Shimpi	6.1276	6.5032	6.9029	9.0930	10.7870	12.5969
		TSDT of Reddy	6.1275	6.3844	6.8312	9.0871	10.3973	11.9011
		Reddy (2004)-Levy	6.128	6.387	6.836	9.087	10.393	11.890
		Reddy (2004)-FEM	6.172	6.192	6.648	9.103	10.582	12.053
	10	Zigzag of Cho	6.9694	7.3031	7.8388	10.6060	12.9660	15.9102
		RPT of Shimpi	6.9438	7.3252	7.8526	10.5778	13.1549	16.3941
		TSDT of Reddy	6.9437	7.2777	7.8116	10.5680	12.8776	15.7354
		Reddy (2004)-Levy	6.943	7.277	7.810	10.568	12.87	15.709
		Reddy (2004)-FEM	6.915	7.134	7.680	10.594	13.180	15.914
5	5	Zigzag of Cho	8.1181	8.2454	8.9215	11.6201	12.4479	13.4879
		RPT of Shimpi	8.1554	8.7424	9.0837	11.6734	12.9985	14.1667
		TSDT of Reddy	8.1554	8.2822	8.9606	11.6730	12.5186	13.5784
		Reddy (2004)-Levy	8.155	8.288	8.996	11.673	12.154	13.568
		Reddy (2004)-FEM	7.989	7.998	8.694	11.664	12.633	13.710
	10	Zigzag of Cho	10.8709	11.0510	11.8389	15.7380	18.1348	20.7864
		RPT of Shimpi	10.8928	11.3455	11.9728	15.7701	18.9060	22.1602
		TSDT of Reddy	10.8928	11.0730	11.8617	15.7701	18.1925	20.8754
		Reddy (2004)-Levy	10.893	11.074	11.863	15.771	18.175	20.831
		Reddy (2004)-FEM	10.906	11.088	11.788	15.787	18.214	20.493

in the number of layers, length to thickness ratios and lamination angle. As observed in Tables 18 and 19, based on different plate theories with different length to thickness ratios the obtained results are in good agreement with other numerical methods.

The effect of lamination angle on the non-dimensional natural frequency is proposed for simply supported angle-ply laminated square plate $[\theta/-\theta]$ with different modulus ratios and length to thickness ratio $a/h = 10$ is diagrammed in Fig. 4(a) and with different length to thickness ratios and with modulus ratio $E_1/E_2 = 40$ in Fig. 4(b) based on TSDT of Reddy, where in Fig. 4(a), an increase in the modulus ratio, increase the non-dimensional natural frequency.

For modulus ratio $E_1/E_2 = 3$, any change in the lamination angle, is of little effect on the non-dimensional natural frequency because its modulus ratio is close to isotropic material properties, while an increase in the modulus ratio, considerably effects lamination angle. As observed in Fig. 4(b), in $\theta = 45°$ constitutes the dominant symmetry of the non-dimensional natural frequency.

4. Conclusions

In the present study, based on different plate theories a finite strip formulation is developed for buckling and free vibration analysis of cross-ply and angle-ply laminated plates. The finite strip procedure based on the virtual work principle is applied to obtain the stiffness, geometric and mass matrices. The accuracy of this formulation is verified by comparing its numerical predictions with the published data. The numerical results indicate a successful gradual convergence and that the zigzag theory and higher other theories are in better accuracy in comparison with CLPT, FSDT, and RPT. It is revealed that the non-dimensional natural frequency in antisymmetric angle-ply plates increases by an increase in the number of layers, length to thickness ratios and lamination angle. Also, in antisymmetric cross-ply plates, an increase in the number of layers increase the non-dimensional buckling load from 2 to 4 layer significantly, while more than 4 this parameter does not change considerably.

The interaction curves for symmetric cross-ply plate with simply supported boundary condition in the longitudinal direction, indicate that when one of the boundary conditions in the transverse direction is fixed or simply supported, due to DOF restrains, the non-dimensional critical buckling load varies linearly, while for a plate of at least one free boundary condition, the same varies nonlinearly.

References

Amoushahi, H. (2018), "Time depended deformation and buckling of viscoelastic thick plates by a fully discretized finite strip method using Third order shear deformation theory", *European J. Mech. A Solids*, **68**, 38–52. https://doi.org/10.1016/j.euromechsol.2017.11.003.

Amoushahi, H. and Goodarzian, F. (2018), "Dynamic and buckling analysis of composite laminated plates with and without strip delamination under hygrothermal effects using finite strip method", *Thin-Walled Struct.*, **131**, 88–101. https://doi.org/10.1016/j.tws.2018.06.030.

Amoushahi, H. and Lajevardi, M.M. (2018), "Buckling of functionally graded plates under thermal, axial, and shear in-plane loading using complex finite strip formulation", *J. Thermal Stresses*, **41**(2), 182–203. https://doi.org/10.1080/01495739.2017.1389326.

Akhras, G. and Li, W. (2007), "Spline finite strip analysis of composite plates based on higher–order zigzag composite plate theory", *Compos. Struct.*, **78**(1), 112–118. https://doi.org/10.1016/j.compstruct.2005.08.016.

Aydogdu, Me. and Aksencer, T. (2018), "Buckling of cross-ply composite plates with linearly varying In-plane loads", *Compos. Struct.*, **183**, 221–231. https://doi.org/10.1016/j.compstruct.2017.02.085.

Bouazza, M., Kenouza, Y., Benseddiq, N. and Zenkour, A.M. (2017), "A two-variable simplified nth-higher-order theory for free vibration behavior of laminated plates", *Compos. Struct.*, **182**, 533–541. https://doi.org/10.1016/j.compstruct.2017.09.041.

Cheung, Y. K. (1968), *Finite Strip Method in Structural Analysis*, Pergamon Press, New York, NY, USA.

Cho, M. and Parmerter, R. (1993), "Efficient higher order composite plate theory for general lamination configurations", *AIAA J.*, **31**(7), 1299–1306. https://doi.org/10.2514/3.11767.

Fallah, N. and Delzendeh, M. (2018), "Free vibration analysis of laminated composite plates using meshless finite volume method", *Eng. Anal. Boundary Elements*, **88**, 132–144. https://doi.org/10.1016/j.enganabound.2017.12.011.

Hosseini-Hashemi, S., Khorshidi, K. and Amabili, M. (2008), "Exact solution for linear buckling of rectangular Mindlin plates", *J. Sound Vib.*, **315**(1), 318–342. https://doi.org/10.1016/j.jsv.2008.01.059.

Karama, M., Afaq, K.S. and Mistou, S. (2003), "Mechanical behaviour of laminated composite beam by the new multi-layered laminated composite structures model with transverse shear stress continuity", *J. Solids Struct.*, **40**(6), 1525–1546. https://doi.org/10.1016/S0020-7683(02)00647-9.

Mechab, I. Mechab, B. and Benaissa, S. (2013) "Static and dynamic analysis of functionally graded plates using four-variable refined plate theory by the new function", *Compos. Part B Eng.*, **45**(1), 748–757. https://doi.org/10.1016/j.compositesb.2012.07.015.

Raghu, P., Rajagopal, A. and Reddy, J.N. (2018), "Nonlocal nonlinear finite element analysis of composite plates using TSDT", *Compos. Struct.*, **185**, 38–50. https://doi.org/10.1016/j.compstruct.2017.10.075.

Reddy, J.N. (2004), *Mechanics of Laminated Composite Plates and Shells: Theory and Analysis*, CRC press, Florida, USA.

Sayyad, A.S., Shinde, B.M. and Ghugal, Y.M. (2016), "Bending, vibration and buckling of laminated composite plates using a simple four variable plate theory", *Latin American J. Solids Struct.*, **13**(3), 516–535. http://dx.doi.org/10.1590/1679-78252241.

Shimpi, R.P. (2002), "Refined plate theory and its variants", *AIAA J.*, **40**(1), 137–146. https://doi.org/10.2514/2.1622.

Singh, D.B. and Singh, B.N. (2017), "New higher order shear deformation theories for free vibration and buckling analysis of laminated and braided composite plates", *J. Mech. Sci.*, **131**, 265–277. https://doi.org/10.1016/j.ijmecsci.2017.06.053.

Sreehari, V.M., George, L.J. and Maiti, D.K. (2016), "Bending and buckling analysis of smart composite plates with and without internal flaw using an inverse hyperbolic shear deformation theory", *Compos. Struct.*, **138**, 64–74. https://doi.org/10.1016/j.compstruct.2015.11.045.

Tanzadeh, H. and Amoushahi, H. (2018), "Buckling and free vibration analysis of piezoelectric laminated composite plates using various plate deformation theories", *European J. Mech. A Solids*, **74**, 242–256. https://doi.org/10.1016/j.euromechsol.2018.11.013.

Tran, L.V., Thai, C.H., Le, H.T., Gan, B.S., Lee, J. and Nguyen-Xuan, H. (2014), "Isogeometric analysis of laminated composite plates based on a four-variable refined plate theory", *Eng. Analysis Boundary Elements*, **47**, 68–81. https://doi.org/10.1016/j.enganabound.2014.05.013.

Touratier, M. (1991), "An efficient standard plate theory", *J. Eng. Sci.,* **29**(8), 901–916. https://doi.org/10.1016/0020-7225(91)90165-Y.

Yang, W., and He, D. (2018), "Bending, free vibration and buckling analyses of anisotropic layered micro-plates based on a new size-dependent model", *Compos. Struct.*, **189**, 137–147. https://doi.org/10.1016/j.compstruct.2017.09.057.

Zenkour, A.M. (2004), "Buckling of fiber–reinforced viscoelastic composite plates using various plate theories", *J. Eng. Math.*, **50**(1), 75–93. https://doi.org/10.1023/B:ENGI.0000042123.94111.35.

CC

Appendix A

The matrices $\mathbf{B}_{im}^{\mathbf{b}\alpha}$ in Eq. (20) according to RPT for $i = 1,3$ are written as

$$\mathbf{B}_{im}^{\mathbf{b}\varepsilon_0} = \begin{bmatrix} N_i'Y_{1m} & N_i'Y_{2m} & 0 & 0 & 0 & 0 & 0 & 0 \\ 0 & 0 & N_iY_{2m}' & N_iY_{1m}' & 0 & 0 & 0 & 0 \\ N_iY_{1m}' & N_iY_{2m}' & N_i'Y_{2m} & N_i'Y_{1m} & 0 & 0 & 0 & 0 \end{bmatrix}_{3\times 8} \quad (A.1)$$

$$\mathbf{B}_{im}^{\mathbf{b}\kappa} = \begin{bmatrix} 0 & 0 & 0 & 0 & -W_i''Y_{1m} & -R_i''Y_{1m} & 0 & 0 \\ 0 & 0 & 0 & 0 & -W_iY_{1m}'' & -R_iY_{1m}'' & 0 & 0 \\ 0 & 0 & 0 & 0 & -2W_i'Y_{1m}' & -2R_i'Y_{1m}' & 0 & 0 \end{bmatrix}_{3\times 8} \quad (A.2)$$

$$\mathbf{B}_{im}^{\mathbf{b}\chi_a} = \begin{bmatrix} 0 & 0 & 0 & 0 & 0 & 0 & W_i''Y_{1m} & R_i''Y_{1m} \\ 0 & 0 & 0 & 0 & 0 & 0 & 0 & 0 \\ 0 & 0 & 0 & 0 & 0 & 0 & W_i'Y_{1m}' & R_i'Y_{1m}' \end{bmatrix}_{3\times 8} \quad (A.3)$$

$$\mathbf{B}_{im}^{\mathbf{b}\chi_b} = \begin{bmatrix} 0 & 0 & 0 & 0 & 0 & 0 & 0 & 0 \\ 0 & 0 & 0 & 0 & 0 & 0 & W_iY_{1m}'' & R_iY_{1m}'' \\ 0 & 0 & 0 & 0 & 0 & 0 & W_i'Y_{1m}' & R_i'Y_{1m}' \end{bmatrix}_{3\times 8} \quad (A.4)$$

and for $i = 2$ as

$$\mathbf{B}_{im}^{\mathbf{b}\varepsilon_0} = \begin{bmatrix} N_i'Y_{1m} & N_i'Y_{2m} & 0 & 0 \\ 0 & 0 & N_iY_{2m}' & N_iY_{1m}' \\ N_iY_{1m}' & N_iY_{2m}' & N_i'Y_{2m} & N_i'Y_{1m} \end{bmatrix}_{3\times 4} \quad (A.5)$$

$$\mathbf{B}_{im}^{\mathbf{b}\kappa} = \mathbf{B}_{im}^{\mathbf{b}\chi_s} = \mathbf{B}_{im}^{\mathbf{b}\chi_b} = \begin{bmatrix} 0 & 0 & 0 & 0 \\ 0 & 0 & 0 & 0 \\ 0 & 0 & 0 & 0 \end{bmatrix}_{3\times 4} \quad (A.6)$$

Table 18 Non–dimensional natural frequency ($\overline{\omega}$) of simply supported angle-ply laminated square plate $[\theta/-\theta]_n$ with $E_1/E_2 = 40$

		$\theta = 5°$		$\theta = 30°$		$\theta = 45°$		
a/h	Method	$n = 1$	$n = 3$	$n = 1$	$n = 3$	$n = 1$	$n = 3$	$n = 4$
4	Zigzag of Cho	8.7199	8.8568	9.6196	10.5016	10.0007	10.798	10.9148
	TSDT of Touratier	8.7559	8.8933	9.5264	10.6126	9.8502	10.9351	11.0401
	TSDT of Reddy	8.7149	8.859	9.4456	10.5572	9.7594	10.895	10.9906
	Reddy (2004)	8.715	8.859	9.446	10.577	9.759	10.895	—
	Bouazza *et al.* (2017)	—	—	—	—	9.7594	—	10.9905
10	Zigzag of Cho	14.2335	14.8468	12.938	18.1073	13.3509	18.936	19.1986
	TSDT of Touratier	14.2426	14.8558	12.8998	18.1731	13.2932	19.0278	19.2744
	TSDT of Reddy	14.2305	14.8483	12.8731	18.1705	13.2631	19.0249	19.2660
	Reddy (2004)	14.23	14.848	12.873	18.17	13.263	19.025	—
	Bouazza *et al.* (2017)	—	—	12.9283	18.3353	13.2631	—	19.3446
20	Zigzag of Cho	16.6569	17.6188	13.8689	21.6209	14.273	22.8376	23.2090
	TSDT of Touratier	16.6593	17.6211	13.8568	21.6471	14.2554	22.8759	23.2402
	TSDT of Reddy	16.6657	17.6194	13.8488	21.6478	14.2463	22.8768	23.2388
	Reddy (2004)	16.656	17.619	13.849	21.648	14.246	22.877	—
	Bouazza *et al.* (2017)	—	—	—	—	14.2463	—	23.2388
50	Zigzag of Cho	17.626	18.752	14.1774	23.0623	14.5769	24.4724	24.8988
	TSDT of Touratier	17.6264	18.7531	14.1753	23.0673	14.5739	24.4799	24.9048
	TSDT of Reddy	17.6258	18.7529	14.174	23.0675	14.5724	24.4802	24.9047
	Reddy (2004)	17.626	18.753	14.174	23.067	14.572	24.48	—
	Bouazza *et al.* (2017)	—	—	—	—	14.572	—	24.9046

Table 19 The non-dimensional natural frequency ($\overline{\omega}$) of simply supported angle-ply laminated square plate $[45/-45/45]$ with $E_1/E_2 = 40$

	a/h				
Theory	5	10	20	50	100
CLPT	17.2082	25.6102	25.7671	25.8115	25.8179
Reddy (2004)	17.207	25.610	25.767	25.811	25.817
FSDT	12.9678	19.5382	23.6921	25.4398	25.7233
Reddy (2004)	12.924	19.521	23.689	25.439	25.723
TSDT of Reddy	13.1309	19.5736	23.6961	25.4399	25.7233
HSDT of Touratier	13.1748	19.5877	23.6996	25.4405	25.7234
HSDT of Afaq	13.2383	19.6153	23.7090	25.4421	25.7239
Reddy (2004)	13.120	19.573	23.696	25.439	25.721
RPT of Shimpi	13.1308	19.5736	23.6961	25.4399	25.7233
RPT of Reddy	13.1308	19.5736	23.6961	25.4399	25.7233
RPT of Touratier	13.1748	19.5876	23.6996	25.4405	25.7234
RPT of Mechab	13.1254	19.5725	23.6960	25.4399	25.7233
Shimpi (2002)-RPT of Reddy	13.130	19.573	23.696	25.439	25.723
Bouazza et al. (2017)-RPT	13.1308	19.5736	23.6961	25.4399	25.7233
Zigzag of Cho	12.5346	19.0202	23.4385	25.3879	25.7098

The matrices $\mathbf{B}_{im}^{\mathbf{s}\beta}$ in Eq. (21) according to RPT for $i = 1,3$ are written as

$$\mathbf{B}_{im}^{\mathbf{s}\gamma_a} = \begin{bmatrix} 0 & 0 & 0 & 0 & 0 & 0 & 0 & 0 \\ 0 & 0 & 0 & 0 & 0 & 0 & W_i'Y_{1m} & R_i'Y_{1m} \end{bmatrix}_{2\times 8} \quad (A.7)$$

$$\mathbf{B}_{im}^{\mathbf{s}\gamma_b} = \begin{bmatrix} 0 & 0 & 0 & 0 & 0 & 0 & W_iY_{1m}' & R_iY_{1m}' \\ 0 & 0 & 0 & 0 & 0 & 0 & 0 & 0 \end{bmatrix}_{2\times 8} \quad (A.8)$$

and for $i = 2$ as

$$\mathbf{B}_{im}^{\mathbf{s}\gamma_a} = \mathbf{B}_{im}^{\mathbf{s}\gamma_b} = \begin{bmatrix} 0 & 0 & 0 & 0 \\ 0 & 0 & 0 & 0 \end{bmatrix}_{2\times 4} \quad (A.9)$$

The matrices $\mathbf{B}_{im}^{\mathbf{b}\alpha}$ in Eq. (20) according to other theories for $i = 1,3$ are written as

$$\mathbf{B}_{im}^{\mathbf{b}\varepsilon_0} = \begin{bmatrix} N_i'Y_{1m} & N_i'Y_{2m} & 0 & 0 & 0 & 0 & 0 & 0 \\ 0 & 0 & N_iY_{2m}' & N_iY_{1m}' & 0 & 0 & 0 & 0 \\ N_iY_{1m}' & N_iY_{2m}' & N_i'Y_{2m} & N_i'Y_{1m} & 0 & 0 & 0 & 0 \end{bmatrix}_{3\times 8} \quad (A.10)$$

$$\mathbf{B}_{im}^{\mathbf{b}\kappa} = \begin{bmatrix} 0 & 0 & 0 & 0 & -W_i''Y_{1m} & -R_i''Y_{1m} & 0 & 0 \\ 0 & 0 & 0 & 0 & -W_iY_{1m}'' & -R_iY_{1m}'' & 0 & 0 \\ 0 & 0 & 0 & 0 & -2W_i'Y_{1m}' & -2R_i'Y_{1m}' & 0 & 0 \end{bmatrix}_{3\times 8} \quad (A.11)$$

$$\mathbf{B}_{im}^{\mathbf{b}\chi_a} = \begin{bmatrix} 0 & 0 & 0 & 0 & 0 & 0 & 0 & N_i'Y_{1m} \\ 0 & 0 & 0 & 0 & 0 & 0 & 0 & 0 \\ 0 & 0 & 0 & 0 & 0 & 0 & 0 & N_iY_{1m}' \end{bmatrix}_{3\times 8} \quad (A.12)$$

$$\mathbf{B}_{im}^{\mathbf{b}\chi_b} = \begin{bmatrix} 0 & 0 & 0 & 0 & 0 & 0 & 0 & 0 \\ 0 & 0 & 0 & 0 & 0 & 0 & 0 & N_iY_{2m}' \\ 0 & 0 & 0 & 0 & 0 & 0 & 0 & N_i'Y_{2m} \end{bmatrix}_{3\times 8} \quad (A.13)$$

$$\mathbf{B}_{im}^{\mathbf{b}\chi_c} = \begin{bmatrix} 0 & 0 & 0 & 0 & 0 & 0 & 0 & N_i'Y_{2m} \\ 0 & 0 & 0 & 0 & 0 & 0 & 0 & 0 \\ 0 & 0 & 0 & 0 & 0 & 0 & 0 & N_iY_{2m}' \end{bmatrix}_{3\times 8} \quad (A.14)$$

$$\mathbf{B}_{im}^{\mathbf{b}\chi_d} = \begin{bmatrix} 0 & 0 & 0 & 0 & 0 & 0 & 0 & 0 \\ 0 & 0 & 0 & 0 & 0 & 0 & N_iY_{1m}' & 0 \\ 0 & 0 & 0 & 0 & 0 & 0 & N_i'Y_{1m} & 0 \end{bmatrix}_{3\times 8} \quad (A.15)$$

and for $i = 2$ as

$$\mathbf{B}_{im}^{\mathbf{b}\varepsilon_0} = \begin{bmatrix} N_i'Y_{1m} & N_i'Y_{2m} & 0 & 0 & 0 & 0 \\ 0 & 0 & N_iY_{2m}' & N_iY_{1m}' & 0 & 0 \\ N_iY_{1m}' & N_iY_{2m}' & N_i'Y_{2m} & N_i'Y_{1m} & 0 & 0 \end{bmatrix}_{3\times 6} \quad (A.16)$$

$$\mathbf{B}_{im}^{\mathbf{b}\kappa} = \begin{bmatrix} 0 & 0 & 0 & 0 & 0 & 0 \\ 0 & 0 & 0 & 0 & 0 & 0 \\ 0 & 0 & 0 & 0 & 0 & 0 \end{bmatrix}_{3\times 6} \quad (A.17)$$

$$\mathbf{B}_{im}^{\mathbf{b}\chi_a} = \begin{bmatrix} 0 & 0 & 0 & 0 & N_i'Y_{1m} & 0 \\ 0 & 0 & 0 & 0 & 0 & 0 \\ 0 & 0 & 0 & 0 & N_iY_{1m}' & 0 \end{bmatrix}_{3\times 6} \quad (A.18)$$

$$\mathbf{B}_{im}^{\mathbf{b}\chi_b} = \begin{bmatrix} 0 & 0 & 0 & 0 & 0 & 0 \\ 0 & 0 & 0 & 0 & 0 & N_iY_{2m}' \\ 0 & 0 & 0 & 0 & 0 & N_i'Y_{2m} \end{bmatrix}_{3\times 6} \quad (A.19)$$

$$\mathbf{B}_{im}^{\mathbf{b}\chi_c} = \begin{bmatrix} 0 & 0 & 0 & 0 & 0 & N_i'Y_{2m} \\ 0 & 0 & 0 & 0 & 0 & 0 \\ 0 & 0 & 0 & 0 & 0 & N_iY_{2m}' \end{bmatrix}_{3\times 6} \quad (A.20)$$

$$\mathbf{B}_{im}^{\mathbf{b}\chi_d} = \begin{bmatrix} 0 & 0 & 0 & 0 & 0 & 0 \\ 0 & 0 & 0 & 0 & N_iY_{1m}' & 0 \\ 0 & 0 & 0 & 0 & N_i'Y_{1m} & 0 \end{bmatrix}_{3\times 6} \quad (A.21)$$

The matrices $\mathbf{B}_{im}^{\mathbf{s}\beta}$ in E1. (21) according to other theories for $i = 1,3$ are written as

$$\mathbf{B}_{im}^{\mathbf{s}\gamma_a} = \begin{bmatrix} 0 & 0 & 0 & 0 & 0 & 0 & 0 & 0 \\ 0 & 0 & 0 & 0 & 0 & 0 & N_iY_{1m} & 0 \end{bmatrix}_{2\times 8} \quad (A.22)$$

$$\mathbf{B}_{im}^{\mathbf{s}\gamma_b} = \begin{bmatrix} 0 & 0 & 0 & 0 & 0 & 0 & 0 & N_iY_{2m} \\ 0 & 0 & 0 & 0 & 0 & 0 & 0 & 0 \end{bmatrix}_{2\times 8} \quad (A.23)$$

$$\mathbf{B}_{im}^{\mathbf{s}\gamma_c} = \begin{bmatrix} 0 & 0 & 0 & 0 & 0 & 0 & 0 & 0 \\ 0 & 0 & 0 & 0 & 0 & 0 & 0 & N_iY_{2m} \end{bmatrix}_{2\times 8} \quad (A.24)$$

$$\mathbf{B}_{im}^{\mathbf{s}\gamma_d} = \begin{bmatrix} 0 & 0 & 0 & 0 & 0 & 0 & N_iY_{1m} & 0 \\ 0 & 0 & 0 & 0 & 0 & 0 & 0 & 0 \end{bmatrix}_{2\times 8} \quad (A.25)$$

and for $i = 2$ as

$$\mathbf{B}_{im}^{\mathbf{s}\gamma_a} = \begin{bmatrix} 0 & 0 & 0 & 0 & 0 & 0 \\ 0 & 0 & 0 & 0 & N_iY_{1m} & 0 \end{bmatrix}_{2\times 6} \quad (A.26)$$

$$\mathbf{B}_{im}^{\mathbf{s}\gamma_b} = \begin{bmatrix} 0 & 0 & 0 & 0 & 0 & N_iY_{2m} \\ 0 & 0 & 0 & 0 & 0 & 0 \end{bmatrix}_{2\times 6} \quad (A.27)$$

$$\mathbf{B}_{im}^{\mathbf{s}\gamma_c} = \begin{bmatrix} 0 & 0 & 0 & 0 & 0 & 0 \\ 0 & 0 & 0 & 0 & 0 & N_iY_{2m} \end{bmatrix}_{2\times 6} \quad (A.28)$$

$$\mathbf{B}_{im}^{\mathbf{s}\gamma_d} = \begin{bmatrix} 0 & 0 & 0 & 0 & N_iY_{1m} & 0 \\ 0 & 0 & 0 & 0 & 0 & 0 \end{bmatrix}_{2\times 6} \quad (A.29)$$

Appendix B

The matrices $\mathbf{B}_{im}^{\mathbf{u}\xi}$, $\mathbf{B}_{im}^{\mathbf{v}\eta}$, $\mathbf{B}_{im}^{\chi}$ and $\mathbf{B}_{im}^{\mathbf{w}\varepsilon_3}$ in Eqs. (33-(36) according to RPT for $i = 1,3$ are written as

$$\mathbf{B}_{im}^{\mathbf{u}\varepsilon_1} = \begin{bmatrix} N_i'Y_{1m} & N_i'Y_{2m} & 0 & 0 & 0 & 0 & 0 & 0 \\ N_iY_{1m}' & N_iY_{2m}' & 0 & 0 & 0 & 0 & 0 & 0 \end{bmatrix}_{2\times 8} \quad (B.1)$$

$$\mathbf{B}_{im}^{\mathbf{u}\kappa_1} = \begin{bmatrix} 0 & 0 & 0 & 0 & -W_i''Y_{1m} & -R_i''Y_{1m} & 0 & 0 \\ 0 & 0 & 0 & 0 & -W_i'Y_{1m}' & -R_i'Y_{1m}' & 0 & 0 \end{bmatrix}_{2\times 8} \quad (B.2)$$

$$\mathbf{B}_{im}^{\mathbf{v}\varepsilon_2} = \begin{bmatrix} 0 & 0 & N_i'Y_{2m} & N_i'Y_{1m} & 0 & 0 & 0 & 0 \\ 0 & 0 & N_iY_{2m}' & N_iY_{1m}' & 0 & 0 & 0 & 0 \end{bmatrix}_{2\times 8} \quad (B.3)$$

$$\mathbf{B}_{im}^{\mathbf{v}\kappa_2} = \begin{bmatrix} 0 & 0 & 0 & 0 & -W_i'Y_{1m}' & -R_i'Y_{1m}' & 0 & 0 \\ 0 & 0 & 0 & 0 & -W_iY_{1m}'' & -R_iY_{1m}'' & 0 & 0 \end{bmatrix}_{2\times 8} \quad (B.4)$$

$$\mathbf{B}_{im}^{\chi_1} = \begin{bmatrix} 0 & 0 & 0 & 0 & 0 & 0 & W_i''Y_{1m} & R_i''Y_{1m} \\ 0 & 0 & 0 & 0 & 0 & 0 & W_i'Y_{1m}' & R_i'Y_{1m}' \end{bmatrix}_{2\times 8} \quad (B.5)$$

$$\mathbf{B}_{im}^{\chi_2} = \begin{bmatrix} 0 & 0 & 0 & 0 & 0 & 0 & W_i'Y_{1m}' & R_i'Y_{1m}' \\ 0 & 0 & 0 & 0 & 0 & 0 & W_iY_{1m}'' & R_iY_{1m}'' \end{bmatrix}_{2\times 8} \quad (B.6)$$

$$\mathbf{B}_{im}^{\mathbf{w}\varepsilon_3} = \begin{bmatrix} 0 & 0 & 0 & 0 & W_i'Y_{1m} & R_i'Y_{1m} & W_i'Y_{1m} & R_i'Y_{1m} \\ 0 & 0 & 0 & 0 & W_iY_{1m}' & R_iY_{1m}' & W_iY_{1m}' & R_iY_{1m}' \end{bmatrix}_{2\times 8} \quad (B.7)$$

and for $i = 2$ as

$$\mathbf{B}_{im}^{\mathbf{u}\varepsilon_1} = \begin{bmatrix} N_i'Y_{1m} & N_i'Y_{2m} & 0 & 0 \\ N_iY_{1m}' & N_iY_{2m}' & 0 & 0 \end{bmatrix}_{2\times 4} \quad (B.8)$$

$$\mathbf{B}_{im}^{\mathbf{v}\varepsilon_2} = \begin{bmatrix} 0 & 0 & N_i'Y_{2m} & N_i'Y_{1m} \\ 0 & 0 & N_iY_{2m}' & N_iY_{1m}' \end{bmatrix}_{2\times 4} \quad (B.9)$$

$$\mathbf{B}_{im}^{\mathbf{u}\kappa_1} = \mathbf{B}_{im}^{\mathbf{v}\kappa_2} = \mathbf{B}_{im}^{\chi_1} = \mathbf{B}_{im}^{\chi_2} = \mathbf{B}_{im}^{\mathbf{w}\varepsilon_3} = \begin{bmatrix} 0 & 0 & 0 & 0 \\ 0 & 0 & 0 & 0 \end{bmatrix}_{2\times 4} \quad (B.10)$$

The matrices $\mathbf{B}_{im}^{\mathbf{u}\xi}$, $\mathbf{B}_{im}^{\mathbf{v}\eta}$, $\mathbf{B}_{im}^{\chi}$ and $\mathbf{B}_{im}^{\mathbf{w}\varepsilon_3}$ in Eqs. (33)-(36) according to other theories for $i = 1,3$ are written as

$$\mathbf{B}_{im}^{\mathbf{u}\varepsilon_1} = \begin{bmatrix} N_i'Y_{1m} & N_i'Y_{2m} & 0 & 0 & 0 & 0 & 0 & 0 \\ N_iY_{1m}' & N_iY_{2m}' & 0 & 0 & 0 & 0 & 0 & 0 \end{bmatrix}_{2\times 8} \quad (B.11)$$

$$\mathbf{B}_{im}^{\mathbf{u}\kappa_1} = \begin{bmatrix} 0 & 0 & 0 & 0 & -W_i''Y_{1m} & -R_i''Y_{1m} & 0 & 0 \\ 0 & 0 & 0 & 0 & -W_i'Y_{1m}' & -R_i'Y_{1m}' & 0 & 0 \end{bmatrix}_{2\times 8} \quad (B.12)$$

$$\mathbf{B}_{im}^{\mathbf{v}\varepsilon_2} = \begin{bmatrix} 0 & 0 & N_i'Y_{2m} & N_i'Y_{1m} & 0 & 0 & 0 & 0 \\ 0 & 0 & N_iY_{2m}' & N_iY_{1m}' & 0 & 0 & 0 & 0 \end{bmatrix}_{2\times 8} \quad (B.13)$$

$$\mathbf{B}_{im}^{\mathbf{v}\kappa_2} = \begin{bmatrix} 0 & 0 & 0 & 0 & -W_i'Y_{1m}' & -R_i'Y_{1m}' & 0 & 0 \\ 0 & 0 & 0 & 0 & -W_iY_{1m}'' & -R_iY_{1m}'' & 0 & 0 \end{bmatrix}_{2\times 8} \quad (B.14)$$

$$\mathbf{B}_{im}^{\chi_1} = \begin{bmatrix} 0 & 0 & 0 & 0 & 0 & 0 & N_i'Y_{1m} & 0 \\ 0 & 0 & 0 & 0 & 0 & 0 & N_iY_{1m}' & 0 \end{bmatrix}_{2\times 8} \quad (B.15)$$

$$\mathbf{B}_{im}^{\chi_2} = \begin{bmatrix} 0 & 0 & 0 & 0 & 0 & 0 & 0 & N_i'Y_{2m} \\ 0 & 0 & 0 & 0 & 0 & 0 & 0 & N_iY_{2m}' \end{bmatrix}_{2\times 8} \quad (B.16)$$

$$\mathbf{B}_{im}^{\mathbf{w}\varepsilon_3} = \begin{bmatrix} 0 & 0 & 0 & 0 & W_i'Y_{1m} & R_i'Y_{1m} & 0 & 0 \\ 0 & 0 & 0 & 0 & W_iY_{1m}' & R_iY_{1m}' & 0 & 0 \end{bmatrix}_{2\times 8} \quad (B.17)$$

and for $i = 2$ as

$$\mathbf{B}_{im}^{\mathbf{u}\varepsilon_1} = \begin{bmatrix} N_i'Y_{1m} & N_i'Y_{2m} & 0 & 0 & 0 & 0 \\ N_iY_{1m}' & N_iY_{2m}' & 0 & 0 & 0 & 0 \end{bmatrix}_{2\times 6} \quad (B.18)$$

$$\mathbf{B}_{im}^{\mathbf{v}\varepsilon_2} = \begin{bmatrix} 0 & 0 & N_i'Y_{2m} & N_i'Y_{1m} & 0 & 0 \\ 0 & 0 & N_iY_{2m}' & N_iY_{1m}' & 0 & 0 \end{bmatrix}_{2\times 6} \quad (B.19)$$

$$\mathbf{B}_{im}^{\chi_1} = \begin{bmatrix} 0 & 0 & 0 & 0 & N_i'Y_{1m} & 0 \\ 0 & 0 & 0 & 0 & N_iY_{1m}' & 0 \end{bmatrix}_{2\times 6} \quad (B.20)$$

$$\mathbf{B}_{im}^{\chi_2} = \begin{bmatrix} 0 & 0 & 0 & 0 & 0 & N_i'Y_{2m} \\ 0 & 0 & 0 & 0 & 0 & N_iY_{2m}' \end{bmatrix}_{2\times 6} \quad (B.21)$$

$$\mathbf{B}_{im}^{\mathbf{u}\kappa_1} = \mathbf{B}_{im}^{\mathbf{v}\kappa_2} = \mathbf{B}_{im}^{\mathbf{w}\varepsilon_3} = \begin{bmatrix} 0 & 0 & 0 & 0 & 0 & 0 \\ 0 & 0 & 0 & 0 & 0 & 0 \end{bmatrix}_{2\times 6} \quad (B.22)$$

Appendix C

The matrices $\mathbf{B}_{im}^{\mathbf{m}\psi}$ in Eq. (39) according to RPT for $i = 1,3$ are written as

$$\mathbf{B}_{im}^{\mathbf{mu}_0} = \begin{bmatrix} N_iY_{1m} & N_iY_{2m} & 0 & 0 & 0 & 0 & 0 & 0 \\ 0 & 0 & N_iY_{2m} & N_iY_{1m} & 0 & 0 & 0 & 0 \end{bmatrix}_{2\times 8} \quad (C.1)$$

$$\mathbf{B}_{im}^{\mathbf{m}\overline{\mathbf{w}}} = \begin{bmatrix} 0 & 0 & 0 & 0 & -W_i'Y_{1m} & -R_i'Y_{1m} & 0 & 0 \\ 0 & 0 & 0 & 0 & -W_iY_{1m}' & -R_iY_{1m}' & 0 & 0 \end{bmatrix}_{2\times 8} \quad (C.2)$$

$$\mathbf{B}_{im}^{\mathbf{m}\overline{\gamma}} = \begin{bmatrix} 0 & 0 & 0 & 0 & 0 & 0 & W_i'Y_{1m} & R_i'Y_{1m} \\ 0 & 0 & 0 & 0 & 0 & 0 & W_iY_{1m}' & R_iY_{1m}' \end{bmatrix}_{2\times 8} \quad (C.3)$$

$$\mathbf{B}_{im}^{\mathbf{mw}} = \begin{bmatrix} 0 & 0 & 0 & 0 & W_iY_{1m} & R_iY_{1m} & W_iY_{1m} & R_iY_{1m} \end{bmatrix}_{1\times 8} \quad (C.4)$$

and for $i = 2$ as

$$\mathbf{B}_{im}^{\mathbf{mu}_0} = \begin{bmatrix} N_iY_{1m} & N_iY_{2m} & 0 & 0 \\ 0 & 0 & N_iY_{2m} & N_iY_{1m} \end{bmatrix}_{2\times 4} \quad (C.5)$$

$$\mathbf{B}_{im}^{\mathbf{m}\overline{\mathbf{w}}} = \mathbf{B}_{im}^{\mathbf{m}\overline{\gamma}} = \begin{bmatrix} 0 & 0 & 0 & 0 \\ 0 & 0 & 0 & 0 \end{bmatrix}_{2\times 4} \quad (C.6)$$

$$\mathbf{B}_{im}^{\mathbf{mw}} = \begin{bmatrix} 0 & 0 & 0 & 0 \end{bmatrix}_{1\times 4} \quad (C.7)$$

The matrices $\mathbf{B}_{im}^{\mathbf{m}\psi}$ in Eq. (39) according to other theories for $i = 1,3$ are written as

$$\mathbf{B}_{im}^{\mathbf{mu}_0} = \begin{bmatrix} N_iY_{1m} & N_iY_{2m} & 0 & 0 & 0 & 0 & 0 & 0 \\ 0 & 0 & N_iY_{2m} & N_iY_{1m} & 0 & 0 & 0 & 0 \end{bmatrix}_{2\times 8} \quad (C.8)$$

$$\mathbf{B}_{im}^{\mathbf{m}\overline{\mathbf{w}}} = \begin{bmatrix} 0 & 0 & 0 & 0 & -W_i'Y_{1m} & -R_i'Y_{1m} & 0 & 0 \\ 0 & 0 & 0 & 0 & -W_iY_{1m}' & -R_iY_{1m}' & 0 & 0 \end{bmatrix}_{2\times 8} \quad (C.9)$$

$$\mathbf{B}_{im}^{\mathbf{m}\overline{\gamma}} = \begin{bmatrix} 0 & 0 & 0 & 0 & 0 & 0 & N_iY_{1m} & 0 \\ 0 & 0 & 0 & 0 & 0 & 0 & 0 & N_iY_{2m} \end{bmatrix}_{2\times 8} \quad (C.10)$$

$$\mathbf{B}_{im}^{\mathbf{mw}} = \begin{bmatrix} 0 & 0 & 0 & 0 & W_iY_{1m} & R_iY_{1m} & 0 & 0 \end{bmatrix}_{1\times 8} \quad (C.11)$$

and for $i = 2$ as

$$\mathbf{B}_{im}^{\mathbf{mu_0}} = \begin{bmatrix} N_iY_{1m} & N_iY_{2m} & 0 & 0 & 0 & 0 \\ 0 & 0 & N_iY_{2m} & N_iY_{1m} & 0 & 0 \end{bmatrix}_{2\times 6} \tag{C.12}$$

$$\mathbf{B}_{im}^{\mathbf{m\overline{w}}} = \begin{bmatrix} 0 & 0 & 0 & 0 & 0 & 0 \\ 0 & 0 & 0 & 0 & 0 & 0 \end{bmatrix}_{2\times 6} \tag{C.13}$$

$$\mathbf{B}_{im}^{\mathbf{m\overline{\gamma}}} = \begin{bmatrix} 0 & 0 & 0 & 0 & N_iY_{1m} & 0 \\ 0 & 0 & 0 & 0 & 0 & N_iY_{2m} \end{bmatrix}_{2\times 6} \tag{C.14}$$

$$\mathbf{B}_{im}^{\mathbf{mw}} = \begin{bmatrix} 0 & 0 & 0 & 0 & 0 & 0 \end{bmatrix}_{1\times 6} \tag{C.15}$$

Appendix D

The matrix $\mathbf{D_b}$ in Eq. (45) according to different plate theories are defined as

$$\begin{cases} \text{For Zigzag theory: } \mathbf{D_b} = \begin{bmatrix} \mathbf{A^b} & \mathbf{B^b} & \mathbf{D^b} & \mathbf{G^b} & \mathbf{L^b} & \mathbf{T^b} \\ & \mathbf{C^b} & \mathbf{E^b} & \mathbf{H^b} & \mathbf{O^b} & \mathbf{U^b} \\ & & \mathbf{F^b} & \mathbf{I^b} & \mathbf{P^b} & \mathbf{V^b} \\ & & & \mathbf{J^b} & \mathbf{R^b} & \mathbf{W^b} \\ & & & & \mathbf{S^b} & \mathbf{X^b} \\ \text{sym.} & & & & & \mathbf{Z^b} \end{bmatrix} \\ \text{For FSDT, HSDT and RPT: } \mathbf{D_b} = \begin{bmatrix} \mathbf{A^b} & \mathbf{B^b} & \mathbf{D^b} & \mathbf{G^b} \\ & \mathbf{C^b} & \mathbf{E^b} & \mathbf{H^b} \\ & & \mathbf{F^b} & \mathbf{I^b} \\ \text{sym.} & & & \mathbf{J^b} \end{bmatrix} \\ \text{For CLPT: } \mathbf{D_b} = \begin{bmatrix} \mathbf{A^b} & \mathbf{B^b} \\ \text{sym.} & \mathbf{C^b} \end{bmatrix} \end{cases} \tag{D.1}$$

The 3×3 matrices in Eq. (D.1) for $i, j = 1,2,6$ could be defined as

$$\begin{cases} \left(\mathbf{A}_{ij}^{\mathbf{b}}, \mathbf{B}_{ij}^{\mathbf{b}}, \mathbf{C}_{ij}^{\mathbf{b}}\right) = \sum_{k=1}^{N} \int_{z_k}^{z_{k+1}} \overline{\mathbf{Q}}_{ij}^{(k)} (1, z, z^2) dz \\ \left(\mathbf{D}_{ij}^{\mathbf{b}}, \mathbf{E}_{ij}^{\mathbf{b}}, \mathbf{F}_{ij}^{\mathbf{b}}\right) = \sum_{k=1}^{N} \int_{z_k}^{z_{k+1}} \overline{\mathbf{Q}}_{ij}^{(k)} F(z)_{11} (1, z, F(z)_{11}) dz \\ \left(\mathbf{G}_{ij}^{\mathbf{b}}, \mathbf{H}_{ij}^{\mathbf{b}}, \mathbf{I}_{ij}^{\mathbf{b}}, \mathbf{J}_{ij}^{\mathbf{b}}\right) = \sum_{k=1}^{N} \int_{z_k}^{z_{k+1}} \overline{\mathbf{Q}}_{ij}^{(k)} F(z)_{22} (1, z, F(z)_{11}, F(z)_{22}) dz \\ \left(\mathbf{L}_{ij}^{\mathbf{b}}, \mathbf{O}_{ij}^{\mathbf{b}}, \mathbf{P}_{ij}^{\mathbf{b}}, \mathbf{R}_{ij}^{\mathbf{b}}, \mathbf{S}_{ij}^{\mathbf{b}}\right) = \sum_{k=1}^{N} \int_{z_k}^{z_{k+1}} \overline{\mathbf{Q}}_{ij}^{(k)} F(z)_{12} (1, z, F(z)_{11}, F(z)_{22}, F(z)_{12}) dz \\ \left(\mathbf{T}_{ij}^{\mathbf{b}}, \mathbf{U}_{ij}^{\mathbf{b}}, \mathbf{V}_{ij}^{\mathbf{b}}, \mathbf{W}_{ij}^{\mathbf{b}}, \mathbf{X}_{ij}^{\mathbf{b}}, \mathbf{Z}_{ij}^{\mathbf{b}}\right) = \sum_{k=1}^{N} \int_{z_k}^{z_{k+1}} \overline{\mathbf{Q}}_{ij}^{(k)} F(z)_{21} (1, z, F(z)_{11}, F(z)_{22}, F(z)_{12}, F(z)_{21}) dz \end{cases} \tag{D.2}$$

Also, N is the number of layers and the matrix $\mathbf{D_s}$ in Eq. (45) according to different plate theories are defined as

$$\begin{cases} \text{For Zigzag theory: } \mathbf{D_s} = \begin{bmatrix} \mathbf{A^s} & \mathbf{B^s} & \mathbf{D^s} & \mathbf{G^s} \\ & \mathbf{C^s} & \mathbf{E^s} & \mathbf{H^s} \\ & & \mathbf{F^s} & \mathbf{I^s} \\ \text{sym.} & & & \mathbf{J^s} \end{bmatrix} \\ \text{For FSDT, HSDT and RPT: } \mathbf{D_s} = \begin{bmatrix} \mathbf{A^s} & \mathbf{B^s} \\ \text{sym.} & \mathbf{C^s} \end{bmatrix} \end{cases} \tag{D.3}$$

The 2×2 matrices in (D.3) for $i, j = 4,5$ could be defined as

$$\begin{cases} \left(\mathbf{A}_{ij}^{\mathbf{s}}\right) = \sum_{k=1}^{N} \int_{z_k}^{z_{k+1}} \overline{\mathbf{Q}}_{ij}^{(k)} (F'(z)_{11})^2 dz \\ \left(\mathbf{B}_{ij}^{\mathbf{s}}, \mathbf{C}_{ij}^{\mathbf{s}}\right) = \sum_{k=1}^{N} \int_{z_k}^{z_{k+1}} \overline{\mathbf{Q}}_{ij}^{(k)} F'(z)_{22} (F'(z)_{11}, F'(z)_{22}) dz \\ \left(\mathbf{D}_{ij}^{\mathbf{s}}, \mathbf{E}_{ij}^{\mathbf{s}}, \mathbf{F}_{ij}^{\mathbf{s}}\right) = \sum_{k=1}^{N} \int_{z_k}^{z_{k+1}} \overline{\mathbf{Q}}_{ij}^{(k)} F'(z)_{12} (F'(z)_{11}, F'(z)_{22}, F'(z)_{12}) dz \\ \left(\mathbf{G}_{ij}^{\mathbf{s}}, \mathbf{H}_{ij}^{\mathbf{s}}, \mathbf{I}_{ij}^{\mathbf{s}}, \mathbf{J}_{ij}^{\mathbf{s}}\right) = \sum_{k=1}^{N} \int_{z_k}^{z_{k+1}} \overline{\mathbf{Q}}_{ij}^{(k)} F'(z)_{21} (F'(z)_{11}, F'(z)_{22}, F'(z)_{12}, F'(z)_{21}) dz \end{cases} \tag{D.4}$$

In (D.4), the prime on F denotes the differentiation with respect to z.

Appendix E.

The matrix $\mathbf{S_u}$ in Eq. (46) according to different plate theories are defined as

$$\begin{cases} \text{For Zigzag theory: } \mathbf{S_u} = \begin{bmatrix} \mathbf{A^{gu}} & \mathbf{B^{gu}} & \mathbf{D^{gu}} & \mathbf{G^{gu}} \\ & \mathbf{C^{gu}} & \mathbf{E^{gu}} & \mathbf{H^{gu}} \\ & & \mathbf{F^{gu}} & \mathbf{I^{gu}} \\ \text{sym.} & & & \mathbf{J^{gu}} \end{bmatrix} \\ \text{For FSDT, HSDT and RPT: } \mathbf{S_u} = \begin{bmatrix} \mathbf{A^{gu}} & \mathbf{B^{gu}} & \mathbf{D^{gu}} \\ & \mathbf{C^{gu}} & \mathbf{E^{gu}} \\ \text{sym.} & & \mathbf{F^{gu}} \end{bmatrix} \\ \text{For CLPT: } \mathbf{S_u} = \begin{bmatrix} \mathbf{A^{gu}} & \mathbf{B^{gu}} \\ \text{sym.} & \mathbf{C^{gu}} \end{bmatrix} \end{cases} \tag{E.1}$$

The 2×2 matrices in (E.1) for $i, j = 1,2$ could be defined as

$$\begin{cases} \left(\mathbf{A}_{ij}^{\mathbf{gu}}, \mathbf{B}_{ij}^{\mathbf{gu}}, \mathbf{C}_{ij}^{\mathbf{gu}}\right) = \sum_{k=1}^{N} \int_{z_k}^{z_{k+1}} \sigma_{\mathbf{0}ij}(1, z, z^2)dz \\ \left(\mathbf{D}_{ij}^{\mathbf{gu}}, \mathbf{E}_{ij}^{\mathbf{gu}}, \mathbf{F}_{ij}^{\mathbf{gu}}\right) = \sum_{k=1}^{N} \int_{z_k}^{z_{k+1}} \sigma_{\mathbf{0}ij}F(z)_{11}(1, z, F(z)_{11})dz \\ \left(\mathbf{G}_{ij}^{\mathbf{gu}}, \mathbf{H}_{ij}^{\mathbf{gu}}, \mathbf{I}_{ij}^{\mathbf{gu}}, \mathbf{J}_{ij}^{\mathbf{gu}}\right) = \sum_{k=1}^{N} \int_{z_k}^{z_{k+1}} \sigma_{\mathbf{0}ij}F(z)_{12}(1, z, F(z)_{11}, F(z)_{12})dz \end{cases} \tag{E.2}$$

Also, the matrix $\mathbf{S_v}$ in Eq. (46) according to different plate theories are defined as

$$\begin{cases} \text{For Zigzag theory: } \mathbf{S_v} = \begin{bmatrix} \mathbf{A^{gv}} & \mathbf{B^{gv}} & \mathbf{D^{gv}} & \mathbf{G^{gv}} \\ & \mathbf{C^{gv}} & \mathbf{E^{gv}} & \mathbf{H^{gv}} \\ & & \mathbf{F^{gv}} & \mathbf{I^{gv}} \\ \text{sym.} & & & \mathbf{J^{gv}} \end{bmatrix} \\ \text{For FSDT, HSDT and RPT: } \mathbf{S_v} = \begin{bmatrix} \mathbf{A^{gv}} & \mathbf{B^{gv}} & \mathbf{D^{gv}} \\ & \mathbf{C^{gv}} & \mathbf{E^{gv}} \\ \text{sym.} & & \mathbf{F^{gv}} \end{bmatrix} \\ \text{For CLPT: } \mathbf{S_v} = \begin{bmatrix} \mathbf{A^{gv}} & \mathbf{B^{gv}} \\ \text{sym.} & \mathbf{C^{gv}} \end{bmatrix} \end{cases} \tag{E.3}$$

The 2×2 matrices in (E.3) for $i, j = 1,2$ could be defined as

$$\begin{cases} \left(\mathbf{A}_{ij}^{\mathbf{gv}}, \mathbf{B}_{ij}^{\mathbf{gv}}, \mathbf{C}_{ij}^{\mathbf{gv}}\right) = \sum_{k=1}^{N} \int_{z_k}^{z_{k+1}} \sigma_{\mathbf{0}ij}(1, z, z^2)dz \\ \left(\mathbf{D}_{ij}^{\mathbf{gv}}, \mathbf{E}_{ij}^{\mathbf{gv}}, \mathbf{F}_{ij}^{\mathbf{gv}}\right) = \sum_{k=1}^{N} \int_{z_k}^{z_{k+1}} \sigma_{\mathbf{0}ij}F(z)_{22}(1, z, F(z)_{22})dz \\ \left(\mathbf{G}_{ij}^{\mathbf{gv}}, \mathbf{H}_{ij}^{\mathbf{gv}}, \mathbf{I}_{ij}^{\mathbf{gv}}, \mathbf{J}_{ij}^{\mathbf{gv}}\right) = \sum_{k=1}^{N} \int_{z_k}^{z_{k+1}} \sigma_{\mathbf{0}ij}F(z)_{21}(1, z, F(z)_{22}, F(z)_{21})dz \end{cases} \tag{E.4}$$

In addition, the matrix $\mathbf{S_w}$ in Eq. (46) according to all plate theories are defined as

$$\mathbf{S_w} = \mathbf{A^{gw}} \tag{E.5}$$

in which, $\mathbf{A^{gw}}$ is the 2×2 matrix for $i, j = 1,2$ that could be defined as

$$\mathbf{A}_{ij}^{\mathbf{gw}} = \sum_{k=1}^{N} \int_{z_k}^{z_{k+1}} \sigma_{\mathbf{0}ij} dz = \begin{bmatrix} n_x & n_{xy} \\ n_{xy} & n_y \end{bmatrix} \tag{E.6}$$

Appendix F.

The matrix $\mathbf{I_{muv}}$ in Eq. (47) according to different plate theories are defined as

$$\begin{cases} \text{For FSDT, HSDT, RPT and Zigzag theories: } \mathbf{I_{muv}} = \begin{bmatrix} \mathbf{A^{m}} & \mathbf{B^{m}} & \mathbf{D^{m}} \\ & \mathbf{C^{m}} & \mathbf{E^{m}} \\ \text{sym.} & & \mathbf{F^{m}} \end{bmatrix} \\ \text{For CLPT: } \mathbf{I_{muv}} = \begin{bmatrix} \mathbf{A^{m}} & \mathbf{B^{m}} \\ \text{sym.} & \mathbf{C^{m}} \end{bmatrix} \end{cases} \tag{F.1}$$

The 2×2 matrices in Eq. (F.1) for $i, j = 1,2$ could be defined as

$$\begin{cases} \left(\mathbf{A}_{ij}^{\mathbf{m}}, \mathbf{B}_{ij}^{\mathbf{m}}, \mathbf{C}_{ij}^{\mathbf{m}}\right) = \sum_{k=1}^{N} \int_{z_k}^{z_{k+1}} \overline{\rho}_{ij} (1, z, z^2) dz \\ \left(\mathbf{D}_{ij}^{\mathbf{m}}, \mathbf{E}_{ij}^{\mathbf{m}}, \mathbf{F}_{ij}^{\mathbf{m}}\right) = \sum_{k=1}^{N} \int_{z_k}^{z_{k+1}} \overline{\rho}_{ij} \mathbf{F}(z) (1, z, \mathbf{F}(z)) dz \end{cases} \tag{F.2}$$

$$\overline{\rho} = \begin{bmatrix} \rho_0 & 0 \\ 0 & \rho_0 \end{bmatrix} \tag{F.3}$$

In addition, the matrix $\mathbf{I_{mw}}$ in Eq. (53) according to all plate theories are defined as

$$\mathbf{I_{mw}} = \rho_0 h \tag{F.4}$$